STREAK CAMERA RECEIVER DEFINITION STUDIES

C B Johnson
ITT/Electro-Optical Products Division
P O Box 3700
Ft Wayne IN 46801

L T Hunkler, Sr
ITT/Aerospace Communications Division
P O Box 3700
Ft Wayne IN 46801

S A Letzring and P Jaanimagi
University of Rochester
Laboratory for Laser Energetics
250 East River Rd
Rochester NY 14623-1299

19SEP90
Final Report for Period 28SEP89-26JUN90

Prepared for
GODDARD SPACE FLIGHT CENTER
Greenbelt MD 20771

(NASA-CR-189251) STREAK CAMERA RECEIVER DEFINITION STUDY Final Technical Report, 28 Sep. 1989 - 26 Jun. 1990 (ITT Electro-Optical Products Div.) 110 p
N92-14330
CSCL 14B G3/35
Unclas
0309730

NASA National Aeronautics and Space Administration

Report Documentation Page

1. Report No.	2. Government Accession No.	3. Recipient's Catalog No.

4. Title and Subtitle

Final Technical Report for Streak Camera Receiver Definition Study

5. Report Date

September 1990

6. Performing Organization Code

7. Author(s)

C B Johnson, L T Hunkler, Sr,
S A Letzring, P Jaanimagi

8. Performing Organization Report No.

10. Work Unit No.

9. Performing Organization Name and Address

ITT Electro-Optical Products Division
3700 East Pontiac Street
P.O. Box 3700
Fort Wayne, IN 46801

11. Contract or Grant No.

NAS5-30735

12. Sponsoring Agency Name and Address

NASA
Goddard Space Flight Center
Greenbelt, MD 20771

13. Type of Report and Period Covered

Final 28Sep89 - 26Jun90

14. Sponsoring Agency Code

15. Supplementary Notes

Author affiliations:

Johnson - ITT Electro-Optical Products Division
Hunkler - ITT Aerospace Communications Division
Letzring/Jaanimagi - University of Rochester

16. Abstract

A dual channel picosecond resolution streak camera receiver system must be space qualified for the GLRS instrument. This study has focused on the requirements and characteristics of the streak camera tube and its associated electronics, with some analysis of the input and output interfaces to the streak camera. The major tradeoffs considered and the baseline streak camera design are discussed. A streak tube design is proposed with an internal high gain microchannel plate, and fiberoptic coupling to a solid-state self-scanned CCD array readout assembly. Concerns regarding the reliability of an avalanche transistor based sweep circuit and the radiation resistance of a CCD camera are highlighted for further study. This report contains a significant bibliography.

17. Key Words (Suggested by Author(s))	18. Distribution Statement
Space-Qualified, Streak Camera, laser ranging, altimeter, picosecond, dual wavelength, GLRS, avalanche transistor, sweep circuit	

19. Security Classif. (of this report)	20. Security Classif. (of this page)	21. No. of pages	22. Price
Unclassified	Unclassified	106	

NASA FORM 1626 OCT 86

TABLE OF CONTENTS

ILLUSTRATIONS

1. INTRODUCTION

Detailed streak camera definition studies have been made as a first step toward full flight qualification of a dual channel picosecond resolution streak camera receiver for the Geoscience Laser Altimeter and Ranging System (GLRS). The overall goals for the GLRS system are described by Cohen, et al[1]. This report also discusses the streak camera receiver requirements as they pertain specifically to the GLRS system, and estimates of the characteristics of the streak camera are given, based upon existing and near-term technological capabilities. Important problem areas are highlighted, and possible corresponding solutions are discussed. The use of a streak camera in a similar ground-based laser altimeter has been reported by Abshire and Kalshoven[2].

Our study began by considering both dual linear scan and dual circular synchroscan types of streak tubes. EGG/Amador Valley Operations (EGG/AVO)[3], Hadland Photonics Limited (HPL)[4] and ITT/EOPD submitted proposals to the Jet Propulsion Laboratory in 1987 for the ruggedization of a streak camera for space use, but no contract was let for this work. A synchroscan type of streak tube, eg a circular scan streak tube, was found in our preliminary study to have some important potential advantages[5],[6],[7],[8]. These involved lower deflection drive power and higher reliability of the tuned sweep circuits. However, this approach has not been developed and refined to the extent of the linear scan approach, and no synchroscan streak camera has demonstrated the adjustable sweep speeds required for GLRS. Furthermore, the small round input spot required by the circular scan approach introduces fundamental space-charge and cathode resistivity limitations. Based upon consideration of these and other factors, we elected to baseline the linear scan approach.

After focusing on the dual linear scan streak tube approach, a large base of useful information was found for making projections of the performance characteristics of this type of streak camera for the GLRS. Several tutorial types of papers are available that describe the basic operating principles of various types of streak tubes and

streak cameras[9],[10],[11],[12],[13],[14],[15],[16]. Suzuki, et al[17] in 1980 presented results of Hamamatsu's development of a compact streak camera having a streak tube with an internal microchannel plate (MCP) electron multiplier, an automatic vidicon readout data acquisition system, and a video analyzer employing a microcomputer. Additional improvements have been made in this industry in the last decade[18]. The requirement for a two channel optical input is not new or unusually difficult, since streak cameras having many more optical input channels are presently being used in the laboratory[19]. Also, the use of an MCP electron multiplier structure inside the streak tube, for achieving single photoelectron sensitivity and high spatial and temporal resolutions, has also been demonstrated by several authors[20],[21],[22]. Streak tubes with internal MCPs have been made by Hamamatsu Photonic Systems Corp (HPSC), ITT/Electro-Optical Products Division (ITT), and Instrument Technology Limited (ITL).

1.1. Technical Overview

The main components of the streak camera are shown in Figs 1.1-1 and 2. During operation two light pulses enter the input optical coupler and interface unit, and are directed to the input fiberoptic window of the streak tube at two locations. The wavelengths at the two locations are 355 nm and 532 nm, respectively. A timing signal from the gate unit opens the electronic shutter in the streak tube immediately before receipt of signal at the streak tube, triggers the sweep circuit and causes beam deflection in the streak tube, and returns the streak tube to a gated-off condition until another measurement cycle begins. The readout camera senses the two streaked images at the output phosphor screen of the streak tube, resulting from the two input signals, and the temporal waveform information is determined after being downlinked. The gain of the streak tube is set by the MCP gain unit, a power supply unit provides high voltages for operation of the streak tube focus, gating and deflection circuits, and low voltages for other circuits, and a streak camera control unit is the master control unit for the streak camera.

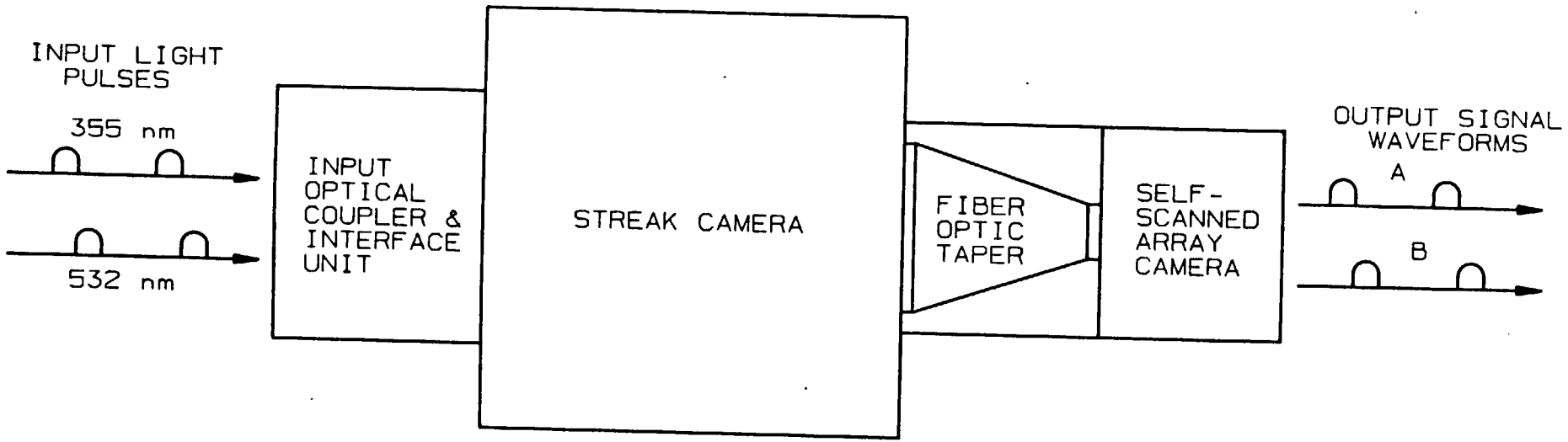

Fig 1.1-1 MAIN COMPONENTS OF GLRS STREAK CAMERA ASSEMBLY

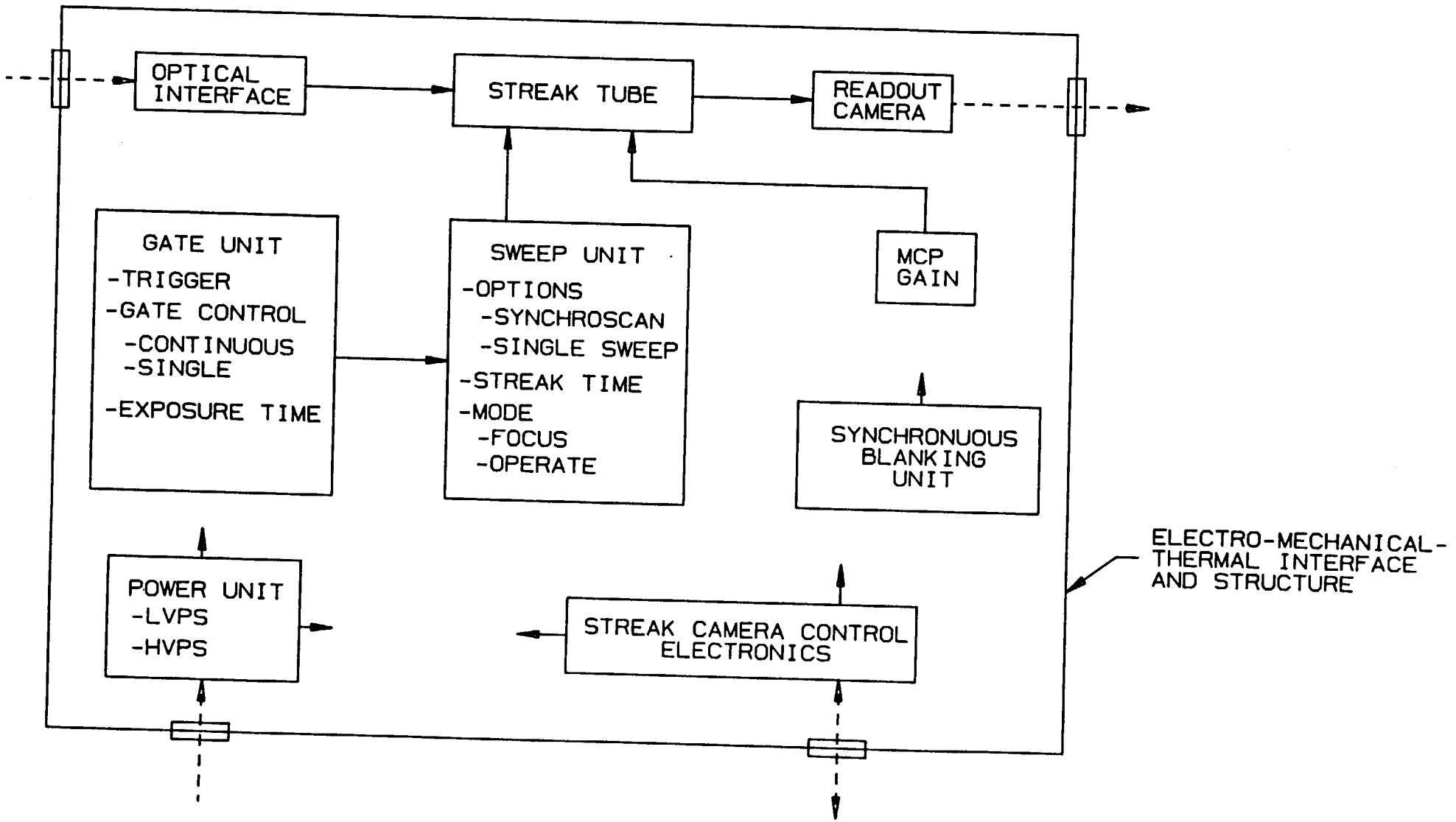

Fig 1.1-2 STREAK CAMERA Block Diagram

The key elements of a streak tube are shown schematically in Fig 1.1-3. In one possible mode of operation, incoming light at the two wavelengths is carried to the input window of the streak tube by individual fibers, and the fiber-to-fiberoptic input window coupling carries the light to the photocathode in the streak tube. Directly adjacent to this photocathode is an electrode (G1) which produces a high electric field at the photocathode, to provide rapid acceleration of the emitted photoelectrons and insure low transit time spread of the electrons from the photocathode to the phosphor screen. Another electrode (G2) and the anode cone electrode (G3) form the electron lens which causes the photoelectrons to be imaged on the phosphor screen. Deflection plates (D' and D") are located in the region between the anode cone and the MCP, and by applying a sawtooth voltage waveform to these electrodes the electrons are deflected across the MCP input in a short time period, eg 1ns. The MCP provides low noise electron gain, and the MCP output signal is proximity focused onto the phosphor screen. Thus the streak tube can be thought of as a time-to-spatial domain transformer; the bright spots located in a line on the screen are the result of successive arrivals of short lightpulses arriving at the photocathode. Beam centering plates (C' and C") are also located between the anode cone electrode and the microchannel plate, and they are used to properly align the electron beamtraces with the readout self-scanned array. Electronic readout is accomplished by fiberoptically coupling the light pattern from the screen to a solid-state self-scanned array. Note that photoelectrons generated by the two input wavelengths are deflected concomitantly, resulting in a dual trace across the screen, and giving the time of arrival information on a common timescale.

Two general types of extraction grid designs can be used in the streak tube, ie a mesh with small openings or a grid or solid electrode with relatively large openings or slots. The mesh type of extraction grid has small square openings in the 18x18 μm^2 to 37x37 μm^2 size range, and having mesh electrical transmissions in the 48% to 60% range. The optical input to the streak tube is not aligned with the mesh openings, and some of the resulting photoelectrons from the cathode

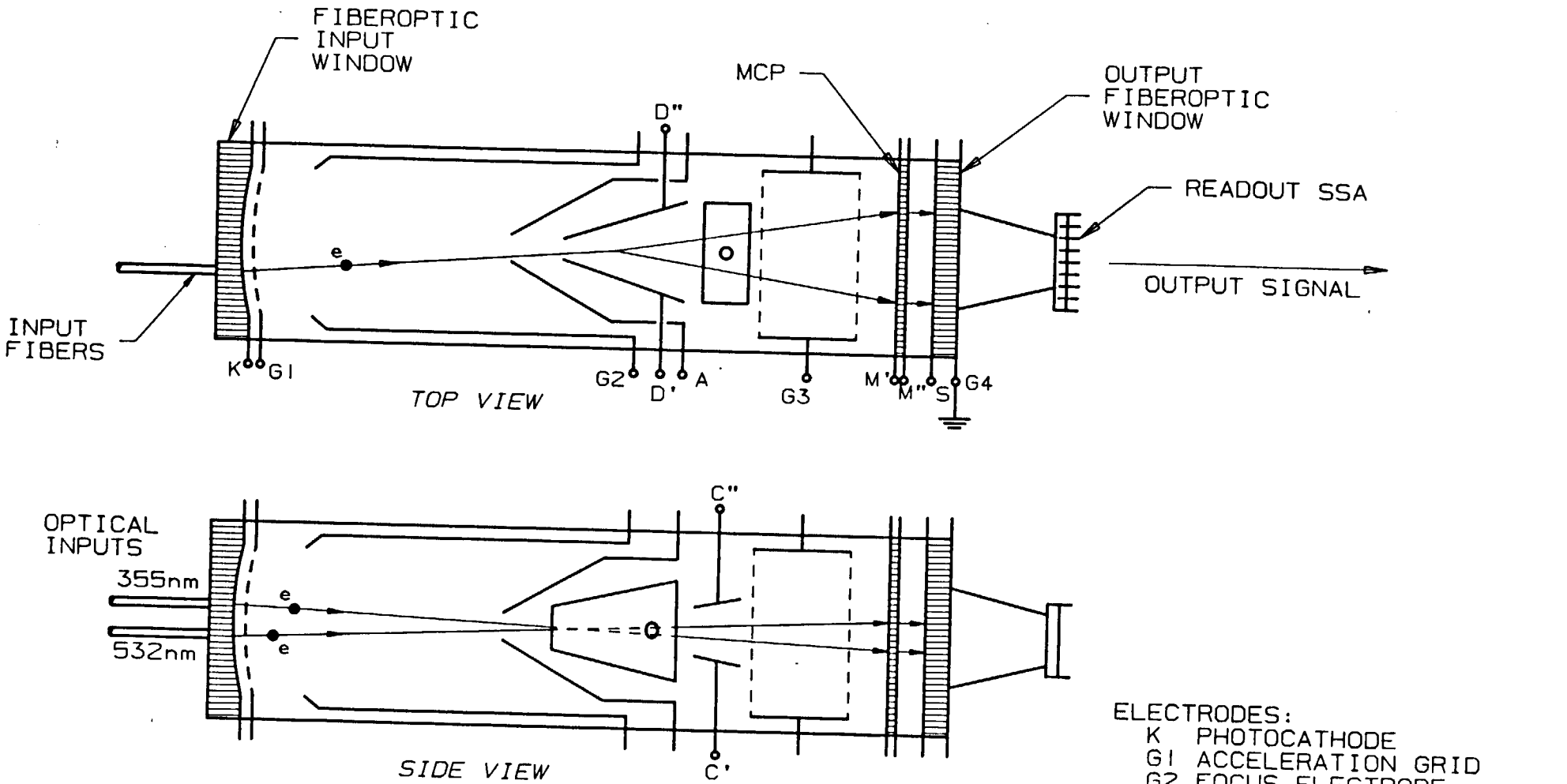

Fig 1.1-3 SCHEMATIC DIAGRAM OF DUAL FIBEROPTIC INPUT LINEAR-SCAN STREAK TUBE WITH INTERNAL MCP AND SOLID-STATE SELF-SCANNED ARRAY READOUT

strike the mesh wires, while some photoelectrons pass through the mesh openings. To a first approximation the photoelectron transmission of the mesh is equal to its optical transmission. Thus, the detective quantum efficiency (DQE) of the cathode fine-mesh design is reduced in proportion to the mesh transmission, which can result in a significant DQE loss. Another disadvantage of a fine mesh extraction grid is that some of the photoelectrons which strike the mesh produce secondary and reflected electrons which result in a spread in the output image, thereby reducing the modulation transfer function (MTF) and causing veiling glare in the streak tube.

Our general recommendation for the acceleration grid design is that its openings should be large enough to allow all of the photoelectrons from a given cathode input channel area to pass through it. In this way there is no signal or DQE loss, loss in MTF, or veiling glare increase from the acceleration grid itself. The larger openings will introduce an electrostatic lens between the cathode and the grid, but the effect of the lenslet at each grid opening can be accommodated by the streak tube's main lens located between the grid and the anode cone. Another important consideration when using the larger acceleration mesh openings is that the optical/photoelectron input regions must be centered on the grid openings, in order to allow good electron-optical imaging within the streak tube. Finally, larger openings also require a larger distance between the cathode and the grid, which introduces a compromise between the size of the grid opening and the electric field strength at the cathode.

Figures 1.1-4 and 5 and Tables 1.1-1 and 2 indicate some of the mechanical, electrical, and performance characteristics of an actual streak tube, ie an ITT #F4157U. Although the #F4157U is designed for a slower speed application, it is an example of a rugged streak tube design whose basic mechanical strength is not compromised when built for 2ps resolution using a microchannel plate. Laboratory streak cameras made by Delli Delti Ltd, Hadland Photonics Ltd and Hamamatsu Photonic Systems Corp are able to achieve the 2 ps time resolution requirement.

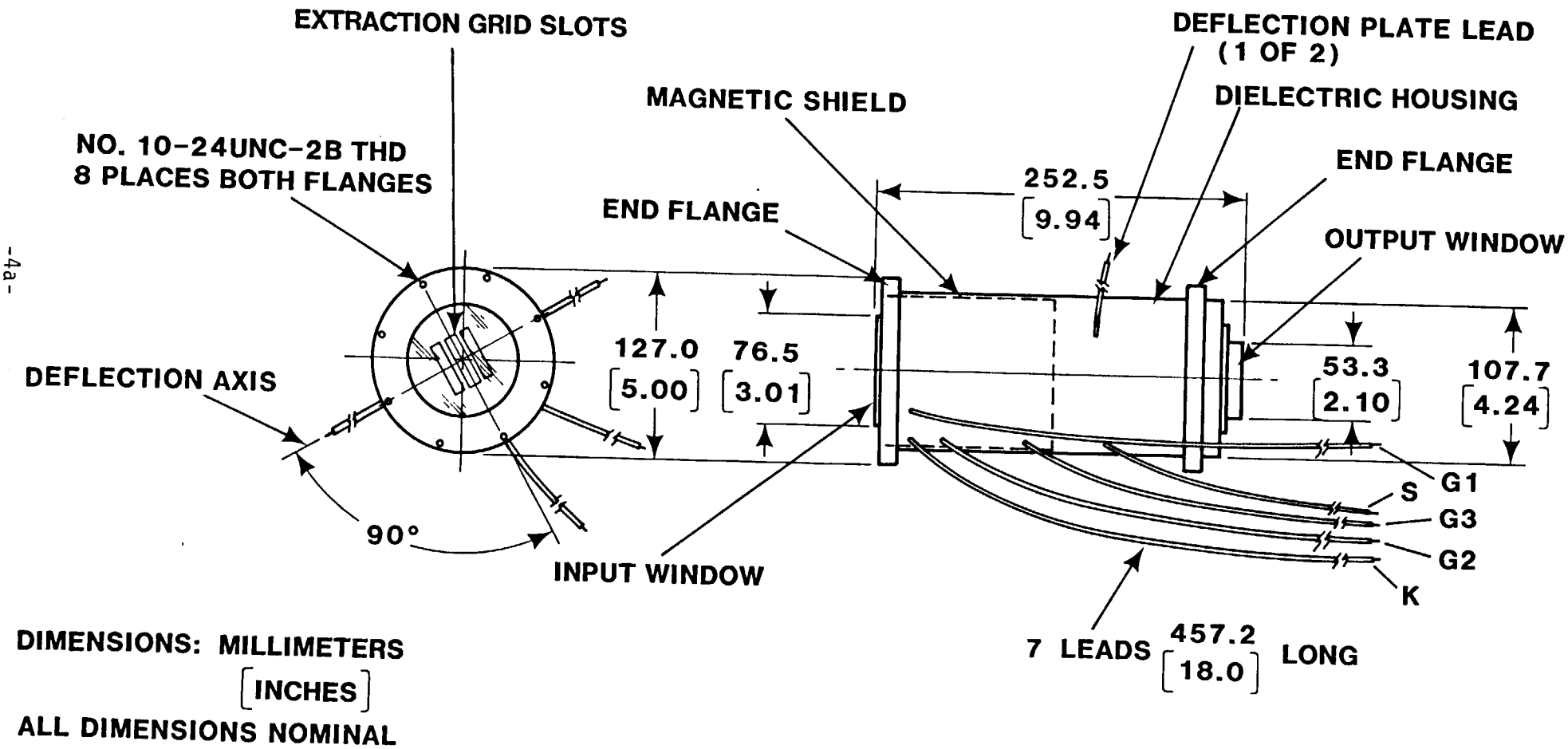

Fig 1.1-4 Sample Streak Tube Potted Assembly
Interface Drawing, ITT Type F4157U

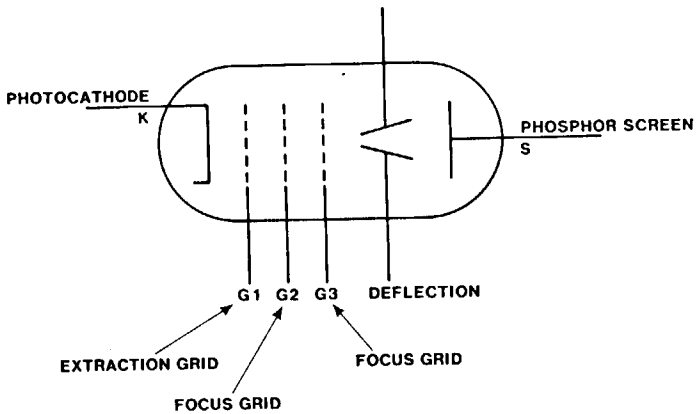

Fig 1.1-5 Sample Streak Tube
Electrical Schematic, ITT Type F4157U

Table 1.1-1

F4157U

PERFORMANCE UNDER TYPICAL OPERATING CONDITIONS

	Minimum	Nominal	Maximum	Units	Notes
Deflection sensitivity	2.4	2.6	2.8	volts/mm/kV	–
Gating Voltage	–	–	– 60	volts	2
Extinction Ratio	1×10^3	–	–	–	3
Temporal Resolution	–	250	–	pico-sec	4
Spatial Resolution	–	–	–	–	5
Axial	35	40	–	lp/mm	
Off-axis, in slot +/– 12mm	10	20	–	lp/mm	–
Axial input, deflected +/– 20mm	8	10	–	lp/mm	–
Off-axis, in slot, +/– 12mm deflected +/– 18mm	–	7	–	lp/mm	–
Magnification					
Axial	–	–	–	–	6
Off-axis, in slot, +/– 12mm	0.75	0.82	0.95	–	–
Axial input deflected +/– 20mm	0.77	0.84	0.97	–	–
Off-axis, in slot, +/– 12mm deflected +/– 18mm	0.77	0.84	0.97	–	–
Photocathode	–	0.88	–	–	–
Quantum Efficiency					
380 nm	11	14	–	percent	–
400 nm	12	15	–	percent	–
Photocathode Uniformity					
400 nm	0.8	–	–	–	7
Radiant Gain					
400 nm	10	–	–	watt/watt	–
EBI					
400 nm	–	1×10^{-13}	1×10^{-10}	watt/cm^2	–

NOTES:

1. All voltages are with respect to the phosphor screen and must be in the stated proportions.
2. G1 to Photocathode for cutoff.
3. Ratio of output screen brightness gated-on to gated-off at 0.02 ft-cd input to the photocathode.
4. Design and development of a New Streak Tube, C.C. Lai, UCAR-10159, Lawrence Livermore National Laboratory, Jun 86.
5. All are visual limiting values at the photocathode under static deflection.
6. All are under static deflection.
7. Ratio of lowest sensitivity area to highest sensitivity area using a 1 mm spot.
8. Average over 1 second interval. May be proportionally higher for pulsed operation.

Table 1.1-2

ABSOLUTE MAXIMUM RATINGS

Temperature		
Non-operating	−20 to +50	Degrees C
Operating	−20 to +40	Degrees C
Voltages (Note 1)		
Photocathode (K)	−16.50	kV
Extraction Grid (G1)	−16.33	kV
Focus Grid (G2)	−16.03	kV
Focus Grid (G3)	−13.63	kV
Phosphor (S)	0	
Deflection	±1.00	kV
Altitude		
Non-Operating	−2000 to +25000	feet
Operating	−2000 to +10000	feet
Input Optical Power (Note 8)		
800 nm equivalent	1×10^{-6}	watt/cm²

TYPICAL OPERATING VOLTAGES at 23 Degrees C (Note 1)

Photocathode (K)	−15.00 kV
Extraction Grid (G1)	−14.85 kV
Focus Grid (G2)	−14.57 kV
Focus Grid (G3)	−12.39 kV
Phosphor (S)	0

G1, G2, G3, voltages shall be adjusted about their nominal values for best electron optical focus.

PHYSICAL SPECIFICATIONS

Mechanical Interface	See Figure 1
Electrical Schematic	See Figure 2
Entrance Window	
Standard	UV transmitting fiber optics
Photocathode	
Standard	High blue response multialkali (MA1). See Figure 3.
Electron Optics	
Type	Five element electrostatic focus
Extraction Grid	Curved, solid cap, concentric with the photocathode, having a 7x35mm slot, and two 5 × 35mm slots.
Deflection Assembly	
Type	Electric field deflection plates single axis
Capacitance	12 pF maximum, to all other electrodes 3 pF maximum, plate to plate
Output Window	
Standard	6 micron EMA fiber optics
Optional	Clear glass
Phosphor Screen	
Standard	Aluminized P20, 44mm minimum diameter area
Optional	Consult manufacturer
Mass	3.5 kg maximum

A conceptual design from Brown[23] for a dual section MCP, with independent gain control in the two sections, is shown in Fig 1.1-6. This design requires that the voltage be held constant across the MCP input to prevent electron lens perturbations. The relatively small voltage differences across the MCP/screen gap are not sufficient to cause noticeable resolution changes. A special type of MCP contact ring would have to be designed in order to use this concept in a practical streak tube. This dual section MCP concept appears to be a viable solution for independently adjusting the pre-readout gain of the two wavelength channels. It is recommended in Section 6 that additional work in this area be carried out during the follow-on program.

1.2. Summary Goal Specifications

This section contains a review of the key performance requirements, along with associated tradeoffs, for the major components of the final flight model streak camera subsystem (FFS). This review is somewhat tutorial, in order to describe the various basic physical limitations and concerns that are the issues of this study. The performance requirements, taken from the SOW, are given and discussed in the following subsections and in Section 2.

1.2.1. Temporal Resolution

* 2 ps FWHM, minimum, in both channels at the single photoelectron level, not to exceed 8 ps FWHM at maximum amplitude

Temporal resolution can be thought of as the result of three major components: input optic "slitwidth" limit (t_s), electron "chromatic" transit-time spread (t_c) in the streak-tube, and the effective "technical" resolution (t_t) of the streak-tube and readout assembly. Simple expressions for these components, useful for physically modeling the performance, can be given using the following definitions, assuming unity streak-tube electron optic magnification:

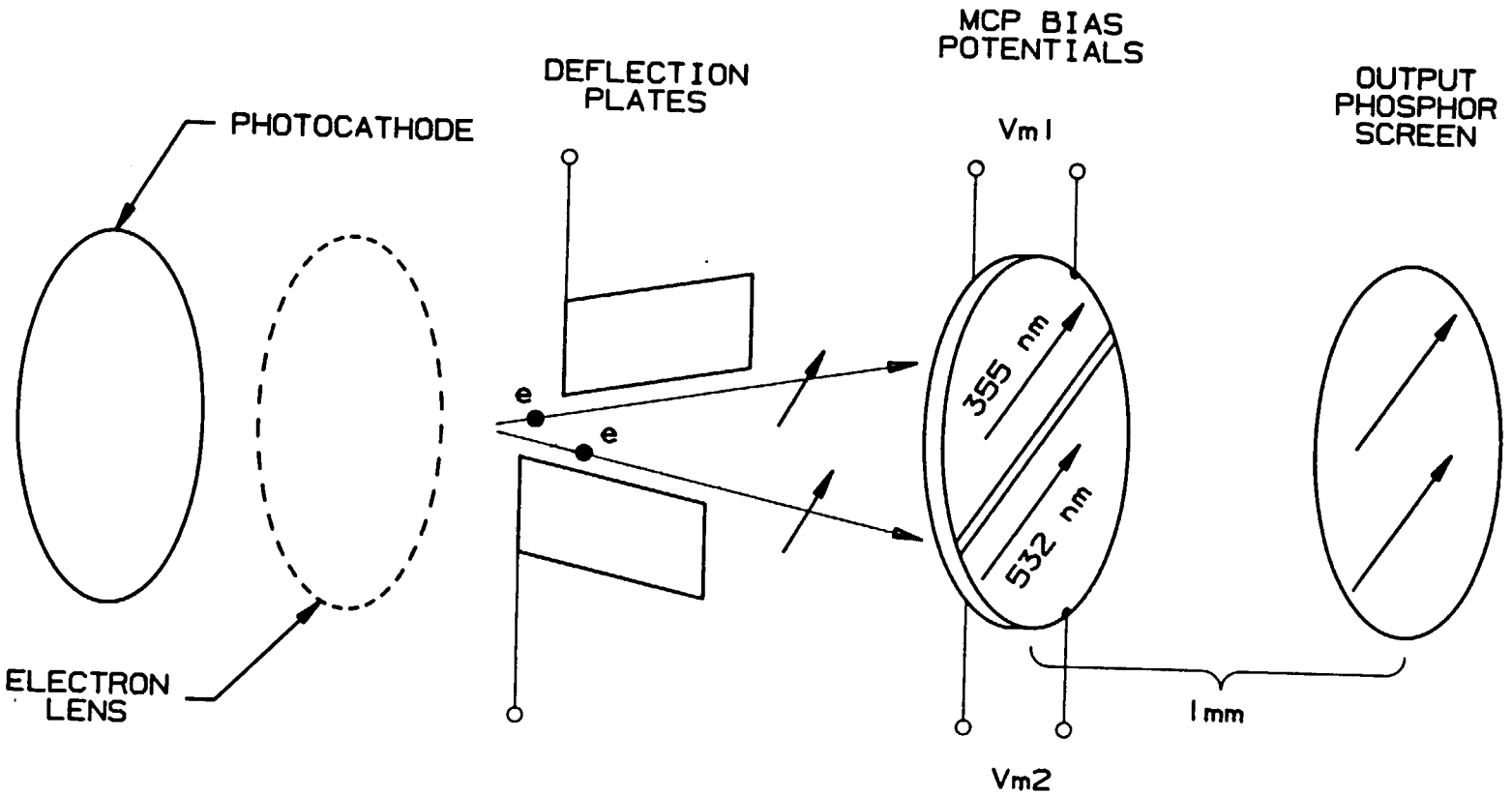

Fig 1.1-6 DUAL ELECTRODE MICROCHANNEL PLATE

dv emitted photoelectron velocity spread,

μ electron charge/mass ratio,

E photocathode electric field strength,

v_s streak velocity at the phosphor screen,

f_l limiting spatial resolution of streak-tube,

W optical input slitwidth,

t_r resultant time dispersion;

$$t_s = W/v_s, \qquad (1.2.1\text{-}1)$$

$$t_c = dv/(uE), \qquad (1.2.1\text{-}2)$$

$$t_t = 1/(v_s f_l), \text{ and} \qquad (1.2.1\text{-}3)$$

$$t_r = \sqrt{(t_s 2 + t_c 2 + t_t 2)}. \qquad (1.2.1\text{-}4)$$

The 2 ps FWHM resolution value can be achieved, for example, with 12 cycle/mm limiting spatial resolution and a streak velocity of 20 mm/500 ps, with all other components being negligible. A more detailed temporal resolution model is given in Appendix 8.1.

One particular laboratory streak camera that does provide less than 2 ps resolution is the HPSC model-C1587 streak camera with the model-M1952 fast single sweep unit. This particular camera and its other characteristics will be referenced again in the appropriate sections.

1.2.2. Input Optical Signals

* 355 nm and 532 nm, recorded simultaneously on each sweep

The input optical signals are within the passband of conventional window/photocathode assemblies, but the required quantum efficiencies are high, based upon present technology. However, the efficiencies depend upon the streak-tube input window material, the photocathode underlayer material and thickness, and the photocathode material and process procedure that are chosen. For example, using uv-fiberoptic windows, no conductive underlayer, and a multialkali photocathode, the maximum sensitivities obtained in ITT type #F4157U streak-tubes are 18% at 355 nm and 11% at 532 nm. Bialkali cathodes alone

probably cannot be used because of poor sensitivity at 532 nm. It is feasible to consider a dual photocathode assembly in a single streak tube, ie having both a bialkali and a multialkali cathodes on the two halves of the input window, as discussed in Section 1.2.4. Also, either conductive underlayers or small active cathode regions surrounded by a conductive film should be used to provide the high current density produced by signal pulses.

Fused silica input window material, and other types of cathodes, should be considered for this application in an effort to meet these performance goals, but the design of the input optical coupling will be directly affected if a fiberoptic input window is not used. It is assumed that a near-uv transmissive input fiberoptic window will be used on the streak tube, in order to reduce the transmission loss at 355nm and provide convenient coupling to either a fiberoptic light guide or an input lens system, although an alternative is discussed in Sections 3 and 4. A sample spectral transmission characteristic of uv fiberoptic window material is given in Fig 1.2.2-1.

1.2.3. Sweep Speeds

* Electrically (digitally) selectable between 0.50-50ns full scale nominal in a 1, 3, 10 sequence

The fastest sweep speed (v_S), ie for the 500 ps sweep period (T_S), will require state-of-the-art circuitry to insure high reliability, but it will probably be possible to meet this requirement in the space-flight qualified streak camera. For example, a streak camera made by HPSC has standard sweep speeds of 0.3, 1, 2, 5, and 10 ns, which meets this requirement in a laboratory streak camera, and the extension to a sweep speed of 50 ns is technically feasible.

1.2.4. Quantum Efficiency

* The goals are 25% at 355 nm and 20% at 532 nm.

The estimated transmission at 355nm is 79.4%. In comparison, the transmission of fused silica at 355nm is 93%.

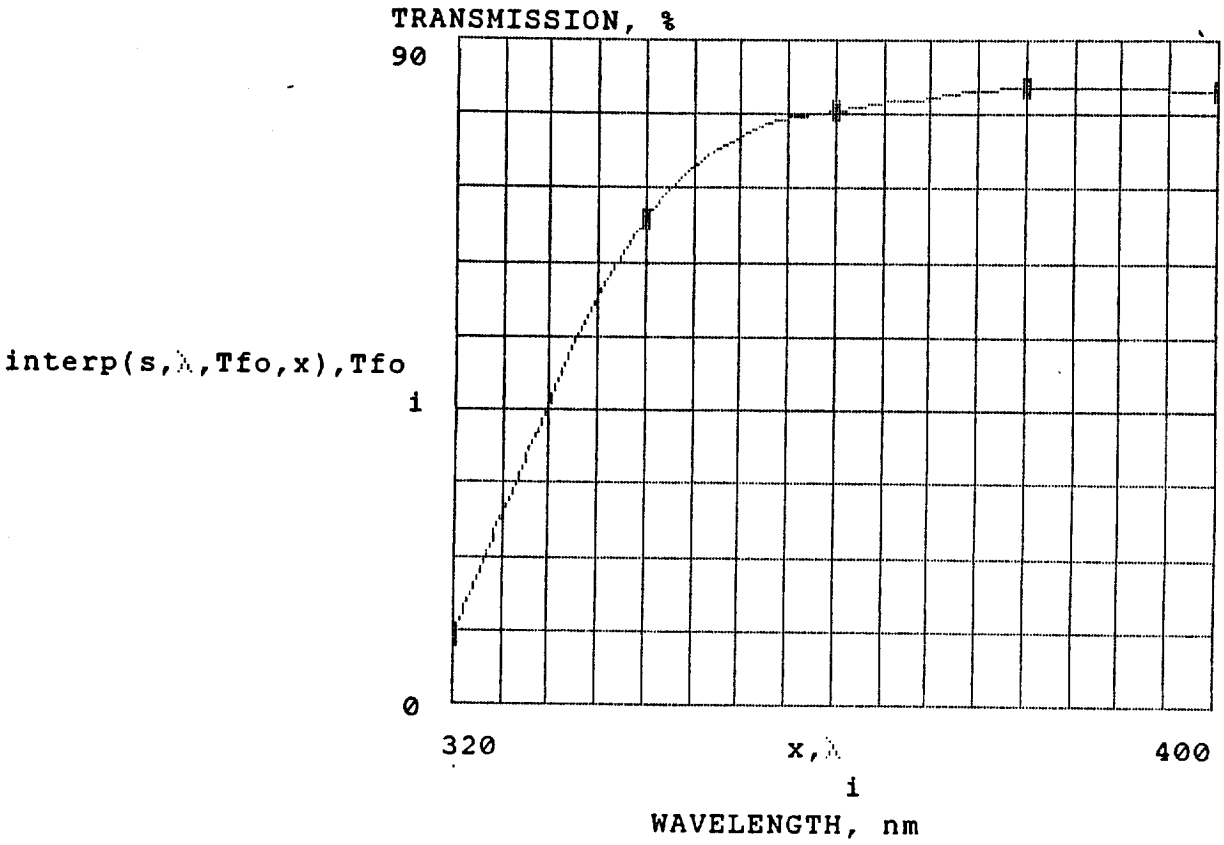

Fig 1.2.2-1 SPECTRAL TRANSMISSION OF 11.7mm THICK INCOM CORP UV FIBEROPTIC WINDOW

The HPSC streak camera does not presently have cathode options that meet these specifications: The streak tube standard product quantum efficiencies are 14% and 9%, respectively. This does not imply, however, that it will be impossible to meet the quantum efficiency goals.

A sample absolute spectral sensitivity curve for an ITT #F4157U streak tube is shown in Fig 1.2.4-1. This tube has a uv transmissive fiberoptic input window and an MA1 photocathode. Its quantum efficiencies are 16% (46 mA/W) and 11% (47 mA/W), respectively, at these two wavelengths. Again the quantum efficiencies fall short of the goals.

Using remote-process methods, it is technically feasible to form a bialkali, eg K-Cs-Sb, photocathode on one half of the input fiberoptic window, for high sensitivity to the 355 nm input signal. The other half can contain a multialkali, eg Na-K-Cs-Sb, photocathode for high sensitivity at 532 nm. This technique will provide higher sensitivity at these two wavelengths than a single photocathode can provide. A review of the maximum sensitivities at these wavelengths indicates that state-of-the-art quantum efficiencies of 28% at 355 nm (fused silica window, ITT type #F4144, #XXC3406) and 16% at 532 nm (fused silica window, ITT type #F4150, #XXN1222) can be achieved, but note that neither of these tubes used uv fiberoptic input windows.

Follow-on work is recommended to better understand the tradeoffs between cathode quantum efficiency, cathode life, and resolution. If a dual cathode is used in the streak tube, the additional dependence of these factors on the cathode processing procedures, possible long-term changes in the two cathodes due to their close proximity to each other, etc, must be determined. The high quantum efficiency of negative electron affinity cathodes, eg GaAs, makes them very attractive for GLRS, but their lifetime and resolution tradeoffs must be determined. These topics are recommended as follow-on tasks in Section 6.

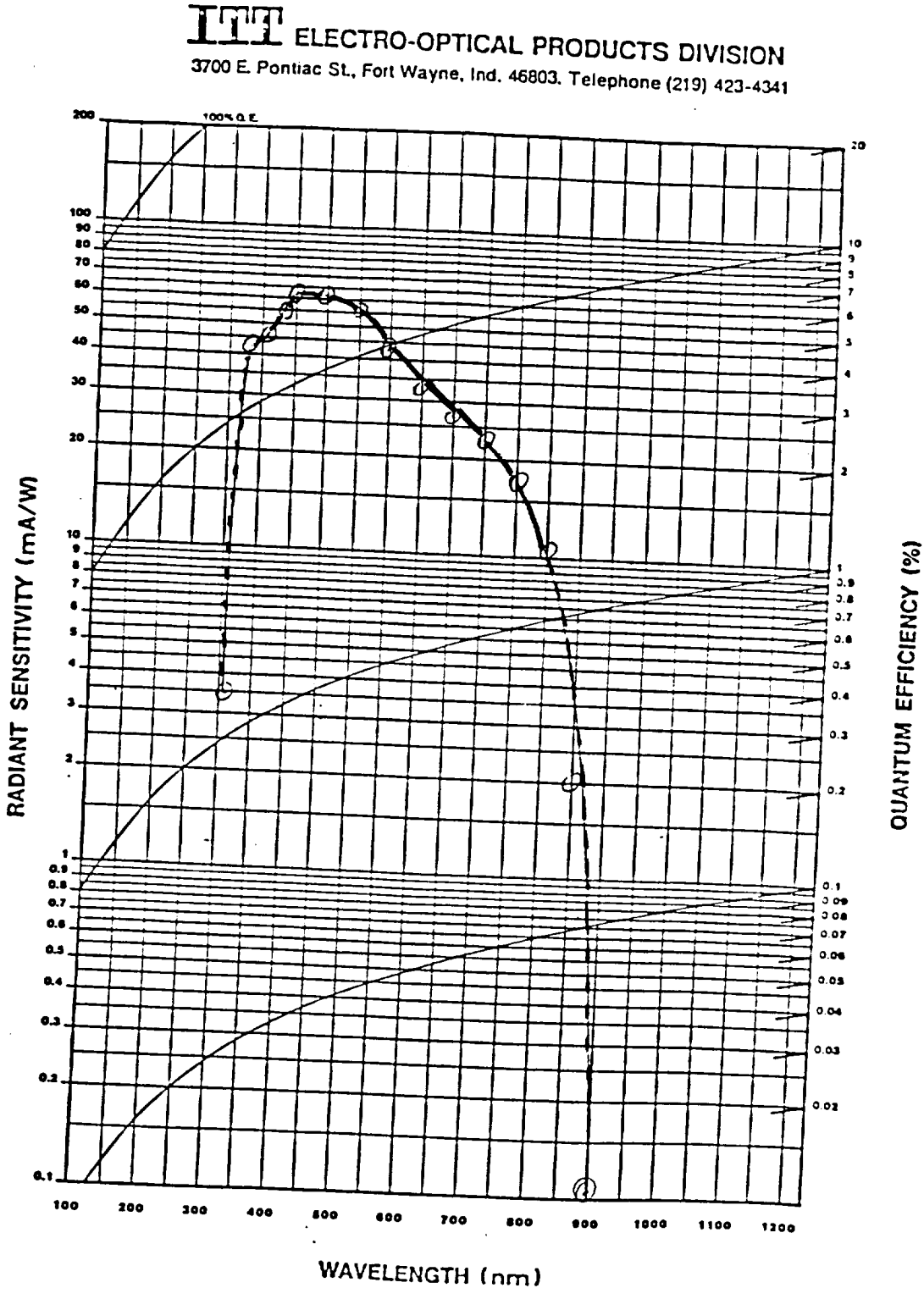

Fig 1.2.4-1 Typical Spectral Sensitivity of a Multialkali Photocathode on a UV Fiberoptic Window

1.2.5. Readout Sensitivity

* single photoelectron/pixel

Single photoelectron/pixel readout sensitivity will be achievable by employing a streak-tube having an MCP with sufficient low noise electron gain to allow a threshold to be set in the self-scanned array (SSA) readout circuit. A curved-channel MCP (CMCP) is recommended for use in the streak tube which has a narrow pulse-height distribution (PHD), for good counting statistics, and high spatial resolution, for high temporal resolution. More discussion of this mode of operation is provided in Sections 1.2.7 and 5 and Appendix 8.2.

In order to achieve photon-counting sensitivity, high pre-readout gain is required. The best presently available technology for achieving low-noise and high gain is to use an MCP electron multiplier either inside or outside of the streak tube. If the MCP is internal to the streak tube a fewer number of image transfer components, and hence higher resolution is achieved. Also, since lower energy input to the MCP is required than to a phosphor screen, higher deflection sensitivity is achieved by using an internal MCP. A broad comparison of the internal and external designs shows that 2 vs 4 fiberoptic windows, 1 vs 2 phosphor screens, 1 vs 2 fiberoptic-to-fiberoptic interfaces, and 1 vs 2 proximity focused sections are required, respectively. The fabrication yield for the internal MCP version is probably higher than the more modular external MCP approach, but the overall advantages seem to be with the internal MCP design.

Conventional MCPs have flat input and output electrode surfaces. Primary photoelectrons which strike the input electrode, ie the web portion of the MCP are either lost and do not contribute to the output signal, or they produce secondaries, some of which can enter the MCP channels and be amplified. The secondaries from the web which enter the MCP will land outside the immediate area of the primary photoelectron, the lateral distance being due to the electric field in the region of the tube in front of the MCP. The confinement and conver-

sion of a larger average number of primary photoelectrons in a small area of the MCP can be achieved by funneling, ie rounding the glass and electrode around each channel. The funneling is achieved by a glass etch process. We recommend the use of a funneled MCP in the streak tube for these reasons.

1.2.6. Amplitude Dynamic Range and Scan Linearity

1.2.6.1. Amplitude Dynamic Range

* 150, minimum, for a given gain setting

An amplitude dynamic range of 150, for a given gain setting, and for and 8 ps, max FWHM timespread pulse, will require that the input optical pulse be a line, and not a small diameter spot, in order to prevent space-charge broadening and cathode resistance limitations. For the highest streak speed the HPSC streak camera only has a dynamic range of 30, which is significantly less than the dynamic range requirement of 150.

A signal-to-noise ratio (R_{sn}) analysis of the streak camera should be made as soon as a candidate design is established. For example, the design proposed in this study could be used to formulate a model and estimate R_{sn} as a reference point to compare future designs and/or design modifications. Signal-to-noise ratio work is a key recommended follow-on task.

1.2.6.2. Scan Linearity

It is recommended that the scan linearity be carefully calibrated before launch, and the components and deflection circuit be designed to be insensitive to component parameter changes[24]. An on-board calibration high speed laser diode and etalon would be a useful addition to the instrument, in order to make routine periodic calibrations of sweep speed and scan linearity. A recalibration should be performed every 1E6 deflections or every month, whichever comes first.

1.2.7. Gain Settings

* electrically adjustable from maximum sensitivity to maximum sensitivity/100 in a 1, 3, 10 sequence

The electrically controlled gain setting requirements, from maximum to maximum/100 values, in a 100, 30, 10, 3, 1 sequence, will be implemented using a digital input. A dedicated #8751 controller will be considered for use in the streak camera for controlling these gain settings, as well as assisting with on-board calibration functions, etc. This is a feasible requirement, and gain will be adjusted by controlling the MCP applied potential.

1.2.8. Switching Speed Between Gain and Sweep Settings

* 25 ms, maximum

A 25 ms switching time period (T_{sw}) between gain and sweep settings is considered to be attainable using an #8751 controller. The controller can switch quickly, but open questions remain concerning how long it will take for the switched circuits to settle to their new value. A model for the recharge-time or dead-time characteristics of MCPs is given by Eberhardt[24A]. A single channel, in a conventional MCP, that releases all of its stored charge is estimated to take about 4 ms to fully recover. The model shows that this recovery time is inversely proportional to the strip current in the MCP. Whereas conventional MCPs have strip current densities of about 1 $\mu A/cm^2$, MCPs are now available with a dc stable strip of 10-20 $\mu A/cm^2$, and pulsed-mode-stable strip current density stable in excess of 100 $\mu A/cm^2$

1.2.9. Gating Pulse

* External TTL or ECL compatible input

The gating pulse circuitry should incorporate the fastest logic available, ie GaAs technology, at the expense of power. This will provide for the least jitter and time delay.

1.2.10. Gate-off Attenuation

* 1000/1 suppression of throughput

The gate-off attenuation value of 1000 is known to be easily attainable in ITT streak-tubes which utilize remotely-processed photocathodes. ITT measurements show that 1E5 is a typical order-of-magnitude attenuation value for streak tubes having remotely processed photocathodes, which is 100x better than required.

1.2.11. Gate Pulse Characteristics

* Minimum width 100 ns nominal, maximum width 20 us nominal

A gate pulse generator, with external TTL compatible input, that will meet the minimum 100 ns gate pulse period (T_g) requirement is already achievable using laboratory equipment. Space qualification of a practical design is judged to be straightforward.

1.2.12. Lifetime

* 1E9 detected pulse pairs during 5 yr operation

Our experience with streak tubes indicates that the main failure component is the photocathode. Also, the photocathode can best be characterized as having a mean-time-to-failure (MTTF), ie a gradual loss of sensitivity, in contrast to other components, eg avalanche transistors, in the streak camera which can best be characterized as having a mean-time-between-failure (MTBF).

It is assumed that the main lifetime limiting mechanism in a streak tube is photocathode degradation, due primarily to ion feedback to the photocathode and the resulting sputtering and/or chemical changes that take place at the photocathode[25]. The worst-case cathode charge loading for a dynamic range of 150 and a maximum input signal of 100 e/pulse is found to be

(150e/e x 100 e/pulse x 1.6E-19 C/e x 1E9 pulse)/(π x 2.52/16)=2.4 $\mu C/cm^2$,

assuming, arbitrarily, that during the course of operation one fourth of a 25 mm diameter cathode is evenly loaded at the maximum input level. This charge density corresponds to an average cathode current density loading over a 5 y period, ie 5y x 365d/y x 24h/d x 3600s/h = 7.9E8s, of 3E-15 A/cm^2, which is only about 8x the cathode dark current density, and thus not of major concern. This estimate applies only during the time that the streak tube is gated-on.

No unusual photocathode life problem is known to exist which would result from normal outgassing inside the tube, assuming that a getter is used and the tube is well electron scrubbed. However, since the streak tube is electrostatically focused, a so-called "ion spot," or reduced sensitivity area in the center of the photocathode due to ion feedback and preferential damage to the photocathode in this region, can be expected to develop over a period of time. Initial testing should make use of the central portion of the cathode before the sensitivity there decays, thus saving the remaining operation for the off-axis area of the photocathode.

Another lifetime limiting factor is associated with the use of avalanche transistors in the streak tube sweep circuit, and this is issue is discussed in Section 2.6.3.

Except for unexpected catastrophic failure of a key component of the streak camera system, the lifetime of 1E9 detected pulse pairs in a 5 yr period is certainly achievable.

1.2.13. Shock, Vibration and Acoustics

Typical of a Martin Marietta Titan-IV launch

The shock, vibration, acoustics, operating and non-operating temperature performance requirements are also judged to be attainable provided that post-launch calibration and alignment procedures are used. Calibration cannot or will not be maintained following the launch environment. The design limit load factors for Earth

Observing System, Polar Orbiting Platform are given in Fig 1.2.13-1, and the preliminary Titan-IV launch vehicle acoustic levels are given in Table 1.2.13-1.

1.2.14. Operating Temperature

* 20±5°C nominal

This is an acceptable operating temperature range for the streak camera. Temperature effects on individual key components, eg circuits, photocathode and phosphor screen, are discussed in Section 2.4.

1.2.15. Non-Operating Temperature

* -30°C to +60°C nominal

This is an acceptable non-operating temperature range for the streak camera. Temperature effects on individual key components, eg circuits, photocathode and phosphor screen, are discussed in Section 2.4.

1.3. Key Results of Study

A simplified streak camera performance model is given in Appendix 8.2. Using this model, in conjunction with the results contained in Section 2, the performance requirements and performance expectations are briefly summarized in Table 1.4-1.

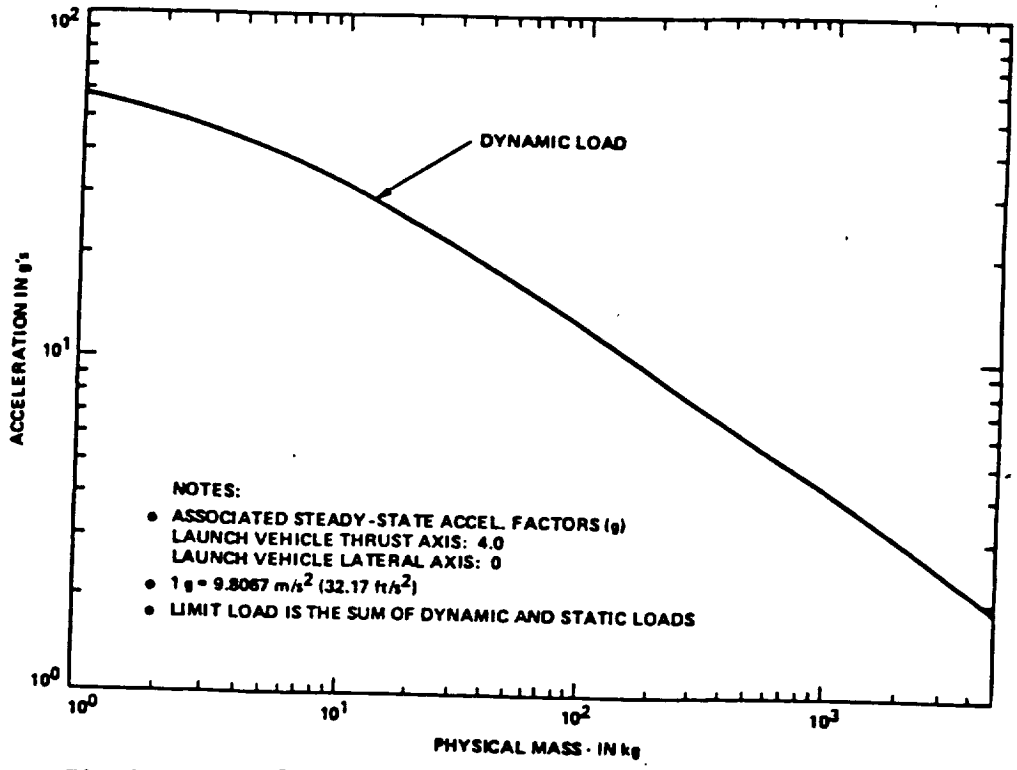

Fig 1.2.13-1 Design Limit Load Factors for Eos POP

Table 1.2.13-1

Preliminary Titan 4 Launch Vehicle Acoustic Levels

FREQUENCY	1/3 OASPL (dB)
31.5	125
40	126.5
50	127
63	128
80	128.5
100	129
125	129
160	129
200	128.5
250	128
315	127.5
400	126.5
500	125.5
630	124.5
800	123
1000	121.5
1250	120.0
1600	118.0
2000	116.5
2500	115.0
3150	113.0
4000	111.5
5000	109.5
6300	107.5
8000	106.0
10000	104.0
	139.3 OVERALL

TABLE 1.4-1 SUMMARY OF PERFORMANCE REQUIREMENTS AND EXPECTATIONS

PARAMETER	REQUIREMENT	EXPECTATION
Temporal Resolution	2ps, FWHM, single photoelectron (PE)	2ps, single PE
Input Optical Signals	355 nm and 532 nm	ok
Sweep Speeds	0.5, 1, 3, 5, 10, 30, 50ns	ok
Quantum Efficiency	25% at 355 nm 20% at 532 nm	25% * 15% *
Readout Sensitivity	Single Photoelectron/Pixel	ok
Amplitude Dynamic Range	150/1 at Each Gain Setting	150/1*
Gain Settings	Settable From Max to Max/100 in 1, 3, 10, 30, 100 Sequence	ok
Switching Speed Between Gain and Sweep Settings	25 ms, Max	ok
Gating Pulse	External TTL or ECL Input	ok
Gate-Off Attenuation	1000/1 Suppression of Throughput	ok
Gate Pulse Characteristics	100 ns min, 20 μs max	ok
Lifetime (5y Operation)	1E9 Detected Pulse Pairs	See Section 2.6
Shock, Vibration, Acoustics	Typical of Titan-IV Launch	ok #
Operating Temperature	20±5°C	ok
Non-Operating Temperature	-30°C to +60°C	ok

NOTES: * Requires state-of-the-art performance and will be difficult to meet.

\# Requires post-launch recalibration.

1.4. Showstoppers

This study has identified one possibly serious problem: The lifetime of the avalanche transistors used in the streak tube deflection circuit. This issue needs immediate attention during the hardware development phase. A more detailed discussion of this issue is given in Section 2.6.3.

2. STUDY AREA RESULTS

Some of the major aspects of the streak camera receiver definition studies are discussed in Appendix 8.2. The remaining methods, techniques and procedures used for these definition studies are described in this report. It has often been possible to give good definition estimates of the key parameters, but in several instances it has been necessary to present only the tradeoffs that might be helpful for making future design choices.

Present laboratory streak cameras having 2 ps resolution capability are available from Delli Delti Ltd (DDL), Hadland Photonics Ltd (HPL), and Hamamatsu Photonics (HPC). The characteristics of these three streak cameras, denoted as DDL, HPL, and HPC, respectively, have been studied in detail and used as a key source of information for this study. It is found that the streak tubes used in these streak cameras are very similar in design, ie they have internally processed cathodes, fine wire mesh acceleration electrodes, plate-on-post deflection plate structures and glass/metal bodies. The unpotted streak tubes used in these streak cameras range from 70-100 mm diameter and 250-350 mm long. The outside diameters of high voltage potted streak tube assemblies are typically 150 mm.

2.1. Size

A smallest practical size estimate has been determined. This estimate is based partly upon estimates from streak camera manufacturers and from our own estimation of the sizes of the individual subassemblies that must be used in the streak camera. The space qualified GLRS streak camera dimensions are expected to be

about the same as for a laboratory streak camera. The mass of the space qualified streak camera will be somewhat larger than standard laboratory streak cameras because of the additional high voltage potting and radiation shielding requirements.

Definitions for the overall outside dimensions of the main components of the streak camera are given in Fig 2.1-1. Rough estimates for the key streak camera (SC) subassemblies are given in Table 2.1-1.

TABLE 2.1-1 SIZE, MASS AND POWER ESTIMATES

	SIZE (l x w x h) (mm x mm x mm)	MASS (kg)	POWER (W)
FIBEROPTIC INPUT UNIT	200 x 175 DIA	2	0
FIBEROPTIC OUTPUT UNIT	80 x 40 DIA	1	0
SSA DRIVE/READOUT-D/A	150 x 50 x 125	1	4
ELECTRONIC INTERFACE UNITS			
TELEMETRY	89 x 165 x 19	0.23	2
LVPS	89 x 165 x 25	0.91	16
COMMAND	89 x 165 x 19	0.23	1
CONTROL	89 x 165 x 19	0.23	2
VIDEO	89 x 165 x 19	0.68	1
DEFLECTION DRIVERS	102 x 127 x 25	0.91	3
HVPS	89 x 165 x 25	0.91	8
MISC CONNECTORS (16)		2.00	
BRACKETS (32)		2.00	
WIRING		0.23	0
POTTING		.23	0
BOX (9 PANELS OF 0.100" ALUM)	2540 x 3632 x 4313	3.27	0
TUBE AND ASSEMBLY	254 x 114 Dia	2.95	2
	2540 x 3632 x 4313 mm^3	18.8 kg	39 W

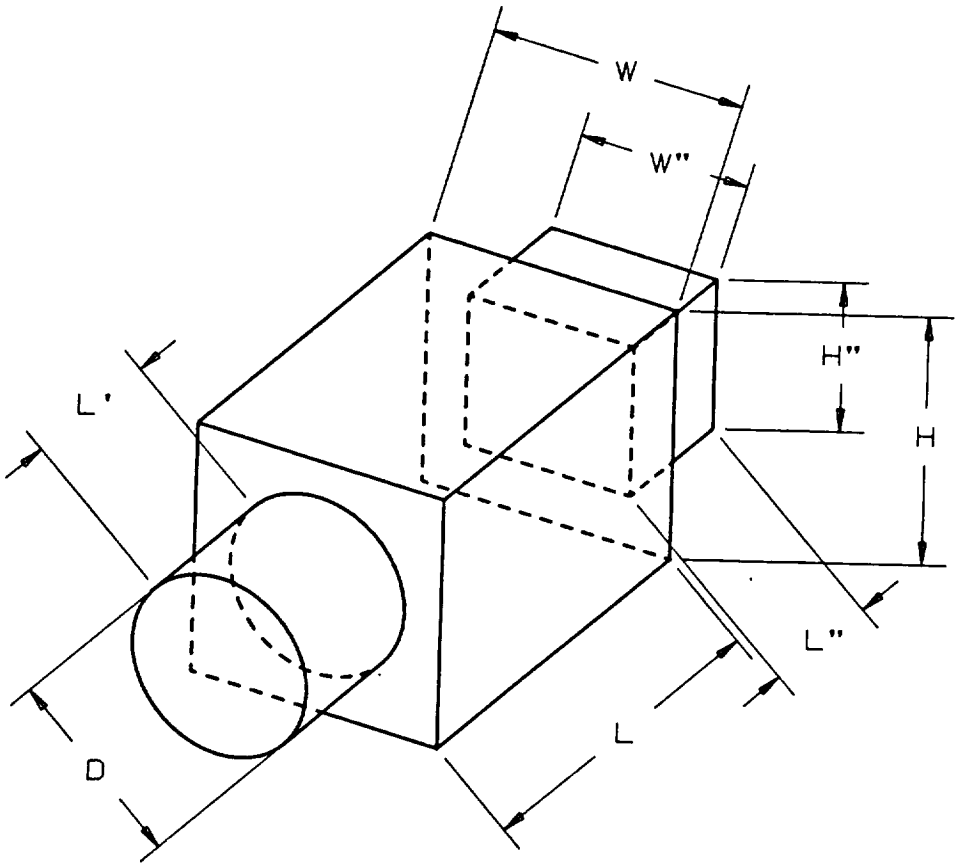

Fig 2.1-1 GLRS STREAK CAMERA DIMENSIONS

A schematic design for the streak camera is shown in Fig 2.1-2, and a preliminary CAD drawing of the streak camera is shown in Fig 2.1-3. The control electronics section will consist of 6 circuit cards or modules containing the same components as used in operational ITT/Aerospace Communications Division (ITT/ACD) instruments. The cards or modules will occupy a volume of 250 x 200 x 100 mm^3 (10" x 8" x 4"). A sensor section will contain the deflection and high voltage power supply modules, along with the streak tube and voltage divider assembly. This sensor section will occupy a volume of 250 x 200 x 140 mm^3 (10" x 8" x 5.5"). It is recommended that these volumes be contained in one unit having a total volume of 250 x 200 x 240 mm^3 (10" x 8" x 9.5"), including spacecraft interfacing connectors. The aluminum box material thickness will be 1-2.5 mm (0.040"-0.100"), depending upon the necessary radiation shielding. This resulting 1.2E4 cm^3 (760 in^3) box volume estimate is similar to that presented at the midterm review at NASA/GSFC on 6MAR90. The final size will also depend upon the ruggedness requirements; a rugged design implies a small size.

This size estimate is compared with another estimate from GE/Astro in Table 2.1-2.

TABLE 2.1-2 SUMMARY OF STREAK CAMERA SIZE ESTIMATES FOR SPACECRAFT INSTRUMENTATION

SOURCE	SIZE (l x w x h) (mm x mm x mm)	COMMENT
GE/ASTRO	350 x 120 DIA	streak camera and readout
	300 x 150 x 150	sweep electronics
STUDY	710 x 300 x 240	

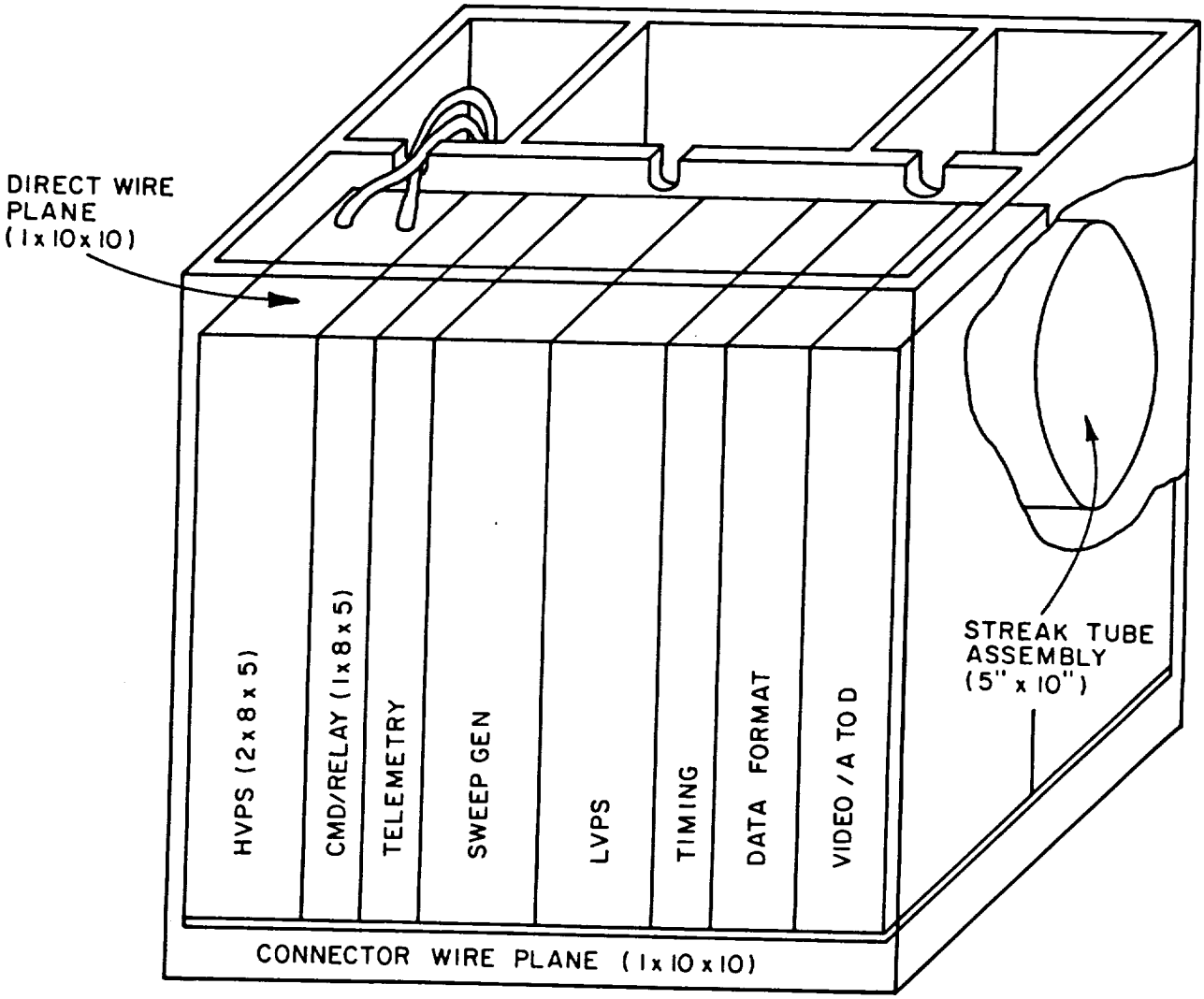

Fig 2.1-2 STREAK SENSOR ASSEMBLY (10" x 10" x 10")

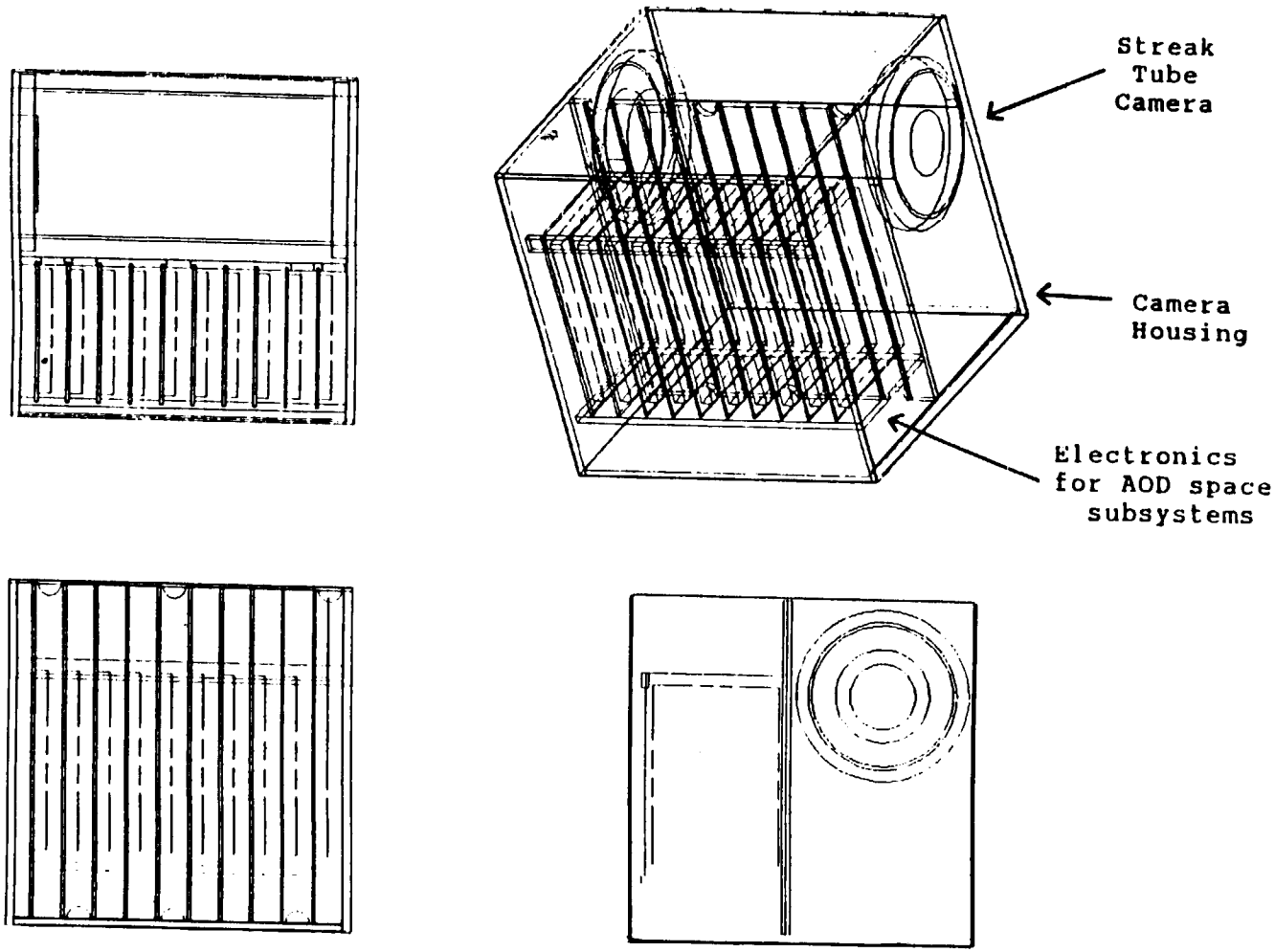

Fig 2.1-3 CAD Drawing of the Streak Camera

2.2. Mass

Wherever possible, and without jeopardizing the performance specifications, our study has focused on finding ways to keep the mass as low as possible. Mass estimates for the individual camera subsystems, and the total mass estimate for the streak camera, are given in Table 2.1-1.

Streak tubes used in the DDL, HPL and HPC streak cameras have masses of about 2 kg (4.4 lbm), and when potted in a magnetic shield and rigid housing with end flanges, the additional mass is about 1kg (2.2 lbm). For maximum strength it is recommended that a metal/ceramic envelope be used in the streak tube. This construction is somewhat more massive than a glass/metal envelope. Both DDL and HPL are available with ceramic/metal streak tubes.

The mass of the 6 circuit cards in the control electronics section, including all connectors, hardware, and the motherboard will be 4.1 lbm, and the mass of the aluminum box will be 3.7 lbm, for a total streak camera electronic system mass of 7.8 lbm. Its base dimensions will be 200 x 200 mm^2, its center of gravity will be (1.4") from this base and close to the geometric center of the box in the other plane.

Assuming 100mil aluminum, the box mass will be approximately (7.2 lbm). This is composed of five (8" x 9"), two (9" x 10") and two (8" x 10") panels. For 40 mil aluminum, the mass will be approximately (5.7 lbm), allowing for support ribs and or braces. The final mass will be a function of the ruggedness and radiation design tradeoffs.

2.3. Ruggedness

There are no known components of the streak camera that are not expected to be rugged enough at this time: However, the streak tube needs to be specially designed to meet the Titan-IV shock and vibration requirements. No commercial streak tube has been qualified to meet these needs. A streak tube manufacturer, not necessarily the manufacturer of the streak camera, should be asked to quote on a ruggedized design which makes maximum use of brazed ceramic/metal streak tube body construction.

Useful reference information on Titan-4 launch and other EOS background data are found in a 1988 NASA Announcement of Opportunity[26]. The preliminary Titan-4 launch vehicle acoustic levels are given in Table 1.2.13-1.

Within the tube assembly we recommend substituting G10 glass epoxy material for acrylic, improving the high voltage wire bonds to the tube, and changing the potting material to Uralane #5753LV, or Conathane #EN11. The high voltage voltage divider will be included in the potted assembly.

We have not performed a complete computer vibration analysis on the streak tube or streak tube assembly. The exact tube component dimensions, mass, and material would first need to be defined. There are many different streak tubes available for analysis, and an analysis of their individual characteristics is beyond the scope of this study.

However, some general comments can be made about the main problem areas and successful solutions to these problems, based upon actual experience on ITT/EOPD and ITT/ACD space programs. This experience has provided approximately 1000 space qualified photoelectronic detectors, with approximately 33% of these actually used in spacecraft, gives us the background for the following discussion.

The use of machined panels and internal bulkheads will will increase the structural rigidity of the streak camera assembly. The ruggedness of the major streak tube subassemblies will need to be carefully designed and qualified; (A) cathode/window/vacuum seal assembly, (B) focus electrode(s), (C) anode-cone and deflection plate assembly, (D) microchannel plate, and (E) phosphor screen/window assembly. These main subassemblies are shown schematically in Fig 1.1-3.

For example, the deflection plate structure in all streak tube designs is of primary concern. Vibration roughly normal to the flat surface of the deflection plates, ie parallel to the deflection direction, will produce deflection and resonances. A simplified vibration model of a deflection plate assembly is shown in Fig 2.3-1 as a mass on the end of a ribbon, with the mass connected to a spring (the deflection plate to lead-out wire). Without damping, the two spring constants are about K1 + K2= 1 kg/mm, and M = 0.1 g for a deflection plate structure in an ITT F4157U streak tube, which results in a resonant frequency of approximately $(1/2\pi)\sqrt{((K1 + K2)/M)}$ = 16 kHz. It is unlikely that a frequency this high will be transmitted through the streak camera structure, so this does not appear to be a major problem. If necessary, this resonant frequency is easily made higher by both changing the location of the lead wire contact point and making the lead-out wire structure more rigid, ie by increasing the spring constant K2.

It is recommended that the streak tube be made using a metal/ceramic brazed vacuum envelope. This type of construction has been found to be more rugged than vacuum envelopes containing large glass/metal seals. Each streak tube supplier has their own type of construction, but all metal/ceramic streak tube designs are rare. EGG/AVO presently makes streak tubes with all metal/ceramic bodies.

After choosing a streak tube design, it must be qualified for space instrument use. Only a remote-process cathode should be used in the streak tube, and In-Bi or In-Sn alloys should be used for the vacuum seal. These types of seal materials have been proven to be very reliable, and they are very tolerant to thermal and mechanical shocks. The remote-process will insure low noise background, high gated-off attenuation, and it is also more rugged than internally processed cathodes.

All of the structural analyses were carried out at ITT/ACD. These analyses were performed on a VAX-3100 using MSC/NASTRAN Solution Sequence 63. Pre- and post-processing were performed with MSC/XL and PDA/PATRAN.

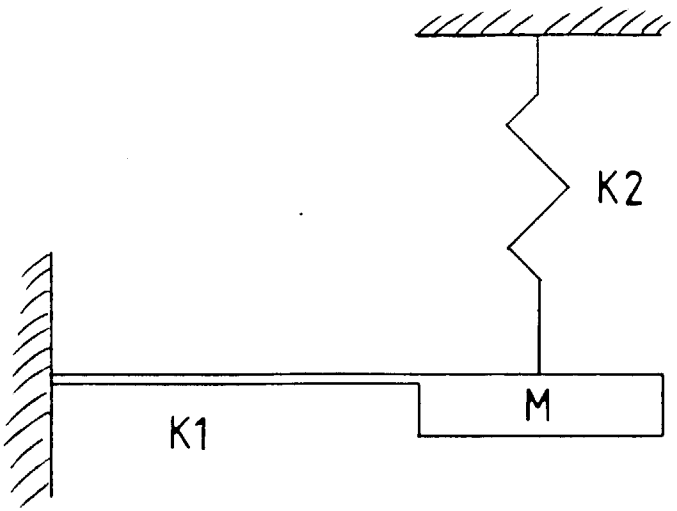

Fig 2.3-1 Simplified Vibration Model of Deflection Plate Structure

Conventional streak tubes are not typically designed for mechanical ruggedness. For GLRS space application, the streak tube's deflection plate structure must be designed to be rugged, and at the same time this structure should also be designed for low deflection plate lead inductance. For example, the proximity focused streak tube developed by Lieber, et al[26A], has a rugged deflection plate structure. Each deflection plate is a single stiff piece of Kovar that is specially shaped, for optimum deflection characteristics. One deflection plate is sealed directly into the glass envelope of the streak tube, and the other one is sealed to a tube body flange. This design also reduces the inductance of the feedthrough, and interconnections from the feedthrough to the deflection plate structure.

Another concept for a deflection plate assembly that would result in a rugged design is to not only seal the deflection plates to the tube envelope, but also make them part of a parallel lead transmission line that passes through the streak tube, and into a matched load. This concept also eliminates ringing and resonance effects in the deflection plate leads, because the distributed inductance and capacitance are part of the transmission line structure.

2.4. Temperature Environment

The maximum temperature range and temperature limiting components have been determined, along with the maximum temperature slew rate, and non-operating temperature limits and durations, and the results are discussed in the following subsections.

2.4.1. Streak Tube

It is recommended that a remote-process photocathode be used in the streak tube for highest quantum efficiency and best uniformity. The final vacuum seal in the streak tube is made between the input window and the tube body using In-Bi or In-Sn eutectic alloys. This type of seal is accomplished inside a vacuum system by (1 holding the molten alloy in a copper retaining ring, (2) moving the input window/cathode assembly into contact with the alloy, (3) rotation of the input

window/cathode assembly to insure good wetting of the alloy to the window, (4) cooling of the tube to room temperature, and (5) removal of the tube from the vacuum system. Since In-Bi is the most common alloy used for remote-process seals, the maximum safe operation or storage temperature is about 65°C. The rest of the streak tube can withstand higher temperatures, and, if necessary, the In-Sn alloy can be used to allow operation up to about 100°C. Of course, the cathode dark current will increase with temperature, as discussed in Section 2.4.3, and state-of-the-art photocathodes are probably not possible.

The melting points of the two commonly used indium alloys, indium-bismuth and indium-tin, for the streak-tube input window seals, for tubes with remote-process cathodes, are 72°C and 116°C, respectively. Temperature considerations are summarized in Table 2.4.1-1.

TABLE 2.4.1-1 SUMMARY OF TEMPERATURE CONSIDERATIONS

MAXIMUM FAILURE TEMPERATURES

STREAK TUBE VACUUM SEAL MATERIALS

In-Bi; 72°C MELTING POINT

In-Sn; 116°C MELTING POINT

(ONLY MOMENTARY HIGH TEMPERATURE EXCURSIONS TO WITHIN 5-10°C OF THESE TEMPERATURES ARE PERMISSIBLE)

MAXIMUM TEMPERATURE SLEW RATE LIMITS

CONTROL ELECTRONICS SYSTEM 5°C/h

The operating and nonoperating temperature ranges for the streak tube are -10 to +50°C and -40 to +110°C, respectively, if In-Sn is used for the vacuum seal material. With a metal/ceramic body, the streak tube will withstand the temperature environmental conditions set by the electronic components discussed in this section. Ideally the operating temperature of the streak camera should be held constant within the range from 0-50°C. There are two concerns for high temperature operation of the streak tube and image intensifier, increased cathode thermionic dark current and reduced photocathode life.

2.4.2. High Voltage Power Supply Environment

Table 2.4.2-1 is an example of specifications that apply to a gateable high voltage power supply for a conventional streak tube, ie ITT type #F4157U. The storage temperature range is -20°C to +50°C, and the operating temperature range for 12% regulation is 20±5°C. It should be located close to the platform for good heat-sinking.

2.4.3. Photocathode Dark Current

The dark current density (Jk) of a Cs-K-Na-Sb multialkali (MA) type of photocathode is given approximately by[27]

$$Jk(Tk)=(4.00E-31)\exp(0.117Tk),\ A/cm^2, \qquad (2.4.4\text{-}1)$$

for -10°C<Tk<40°C, where Tk in equation (2.4.4-1) is the cathode temperature in K. The dark current density of a Cs-K-Sb bialkali photocathode is about fifty to one hundred times less.

2.4.4. Phosphor Screen Persistence

Low temperature operation causes increased persistence in KA (P20) and other types of screen materials. This effect can limit the readout repetition rate for the camera. A faster phosphor material, eg GH (P31), can be used, but the tradeoff with its coupling efficiency to the readout assembly must also be considered. Persistence, peak wavelength and efficiency of several commonly used phosphor screen materials are given in Table 2.4.3-1 for reference. The final choice of the phosphor screen material must be based upon its persistence, efficiency, and spectral matching to the SSA readout array. The screen's reciprocity characteristics must also be verified before using it in the streak tube. One of the authors (P Jaanimagi) has found that P20 screens exhibit reciprocity failure in the ms to ps time ranges, but that P46 and P47 screens appear to maintain good reciprocity characteristics. Also, Cromwell[27A] has reported that the counting efficiency of phosphor screens are generally very low, but that refinements in the manufacture of phosphor screens can yield counting efficiency improvements.

Table 2.4.2-1 Preliminary Specifications for a Space Qualified Streak Camera High Voltage Power Supply

KM electronics·inc 123 INTERSTATE DR·WEST SPRINGFIELD·MASS·01089(413)781-1350

GND ANODE GATEABLE IMAGE TUBE PWR SUPPLY

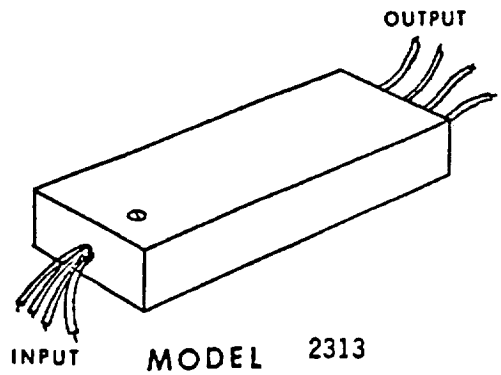

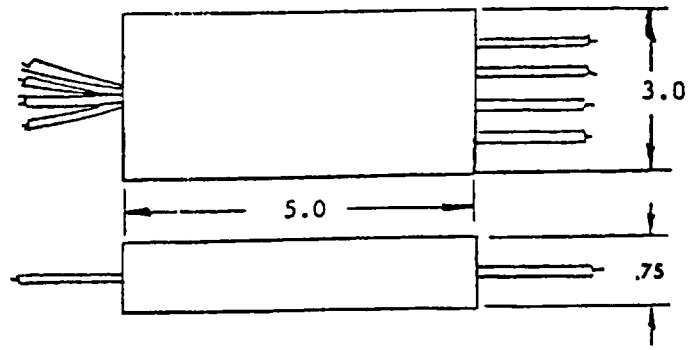

DIMENSIONS ARE IN INCHES

SPECIFICATIONS

Parameter	Name	Min	Nom	Max	Units	Notes	Remarks
Input Voltage	B+	22	28	34	+VDC		
Input Current	I-in	-	-	TBD	mA		
Gate On	EgOn	4.5	-	5.5	+VDC		
Gate Off	EgOff	0	-	.5	+VDC		
Cathode	VK	16.0	16.5	17.0	-KVDC		
G1 Operating	G1-On	160	170	180	+VDC	1	Ref to VK
G1 Gated Off	G1-Off	50	60	70	-VDC	1	Ref to VK
G1 Rise/Fall	tr/tf	-	-	100	nSec		10 to 90%
Eg to G1 Delay	td	-	-	200	nSec		50 to 50%
On Time	PW	100	-	Inf	nSec		50 to 50%
Gating Rep Rate	PRR	0	-	50	Hz		
G2 Minimum	G2 Min	-	-	370	+VDC	1,2	Ref to VK
G2 Maximum	G2 Max	570	-	-	+VDC	1,2	Ref to VK
G3	G3	2840	2900	2960	+VDC	1	Ref to VK
Screen (Anode)	VA	-	0	-	VDC		At B- potential
Line Regulation		-2	-	+2	%		All Outputs
Load Current	IL	-	-	1	uA		
Load Regulation		-2	-	+2	%		
Ripple		-	-	2	%		All Outputs
Operating Temp	To	+15	-	+25	C		
Storage Temp	Ts	-20	-	+50	C		
Operating Pressure		-	10^-7	-	torr		

Notes:
1. Tracks any changes in the cathode voltage within 0.1%.
2. Adjustable via internal potentiometer.

3/23/90

Pg 1 of 1

Table 2.4.3-1

PHOS
32959.
900327
CBJ

PHOSPHOR SCREEN CHARACTERISTICS
REFERENCES: EIA PUBLICATION #116-A, DEC85, & ITT WALL CHART

TYPE..... NEW	OLD	PERSISTANCE..... 50% (s)	20%	10%	WAVELENGTH.... MIN (nm)	MAX	PEAK	EFFICIENCY..... ABS Wr/We	QNTUM p/eV	LUM'S lm/Wr	CLR
BH	P47	2.5E-8	5.7E-8	1.1E-7		400		0.07		65	VB
AA	P16	3.0E-8	7.0E-8	1.2E-7			380	0.05		2.7	VUV
KG	P46	4.8E-8	1.1E-7	1.6E-7		540		0.01		520	YG
KF	P36	5.5E-8	1.5E-7	2.5E-7		550					YG
GE	P24	8.0E-8	5.0E-7	1.6E-6		505		0.024		360	G
GG	P15	2.5E-6	1.2E-6	2.8E-6	390	530		0.044		11	G
GH	P31	4.0E-6	1.8E-5	3.5E-7		520		0.06		420	G
KA	P20	1.0E-4	5.6E-4			560		0.14	0.063	480	YG
GX	P44	3.0E-4	8.0E-4	1.2E-3			540				YG

Whether used in the streak tube or an external image intensifier tube, a portion of any follow-on work should include a more detailed analysis of phosphor screen effects.

2.4.5. Other Temperature Considerations

Steps must also be taken to prevent film deposition, condensation and/or fogging of optical windows or other elements at low temperatures. The non-operating high and low temperature limits are determined by the vacuum envelope integrity of the streak tube and associated optics and optical couplings. Selected areas of the subsystem optics will need heaters to raise their temperatures. This will be determined by the outgassing environment. Most of the circuits should be operated in the 15-25°C range. A current materials list of the streak camera, as well as the entire spacecraft, must be maintained and monitored.

2.4.6. Self-Scanned Array Dark Current

High temperature operation of a self-scanned array (SSA) is of concern also, because its dark current density (Ja) increases with its operating temperature (Ta), causing charge accumulation in the pixel wells, and reduced signal/noise ratio can result if long storage periods between readouts occur. An approximate expression for silicon SSAs is

$$Ja\ (Ta) = (6.6E10)\ \exp\ (-1.3E4/Ta),\ A/cm^2,$$

where Ta is given in K. For example, Ja = 5 nA/cm^2 at Ta = 295 K.

2.4.7. Circuits

Circuits and electronic subassemblies selected by ITT/ACD for space instrument use are typically qualified for baseplate temperatures in the -10 to 40°C range, for operation at a baseplate temperature of 20 ± 5°C. The non-operating storage temperature range will be -20 to +60°C to accommodate the launch pad environment. The temperature rise from the streak camera electronic system box to the

baseplate, while operating, will be about 10°C. A typical and expected temperature rate-of-change is 5°C/h, which is the qualification rate used for ITT/ACD instruments. During holding orbits, in preparation for transfer to planned orbits, the spacecraft baseplate may be near 0°C, and non-operating instruments may receive "cold-soaking" of approximately -10°C, which is well within the storage temperature range. All thermal analyses were calculated at ITT/ACD.

2.4.8. Potting Materials

A material like Conap EN-11 is often used for high voltage space instrumentation because it has a low outgassing characteristic. However, this material becomes very hard when cooled, and some electronic components have been linear thermal expansions. Appropriate buffer coatings, such as those often used on circuit board components, must be incorporated where temperatures drop below 0°C.

2.5. Radiation Environment

The effects of the expected radiation on lifetime, and the tradeoff with shielding have been determined for operation of the streak camera in the proposed 824 km circular polar orbit.

2.5.1. Expected Radiation Environment

In this orbit the streak camera will encounter an average orbital flux of 700 e/cm^2/s, similar to the HIRS, AVHIR, IDCS, HRIR and HCMR operating environments. Using the radiation analysis results of Stassinopolus[28], as shown in Fig 2.5.1-1, and assuming the use of 100 mil Al shielding, it is estimated that this flux will produce a radiation dose of 3500 rad(Si) during a 5 yr period. Another estimate, shown in Fig 2.5.1-2, from NASA/JPL[29], for the 824 km polar orbit is that the total ionizing dose with 100mil Al shielding will be 1E4rad(Si) for a 5 yr period. All components used in the streak camera electronic system have been selected and shielded for this environment.

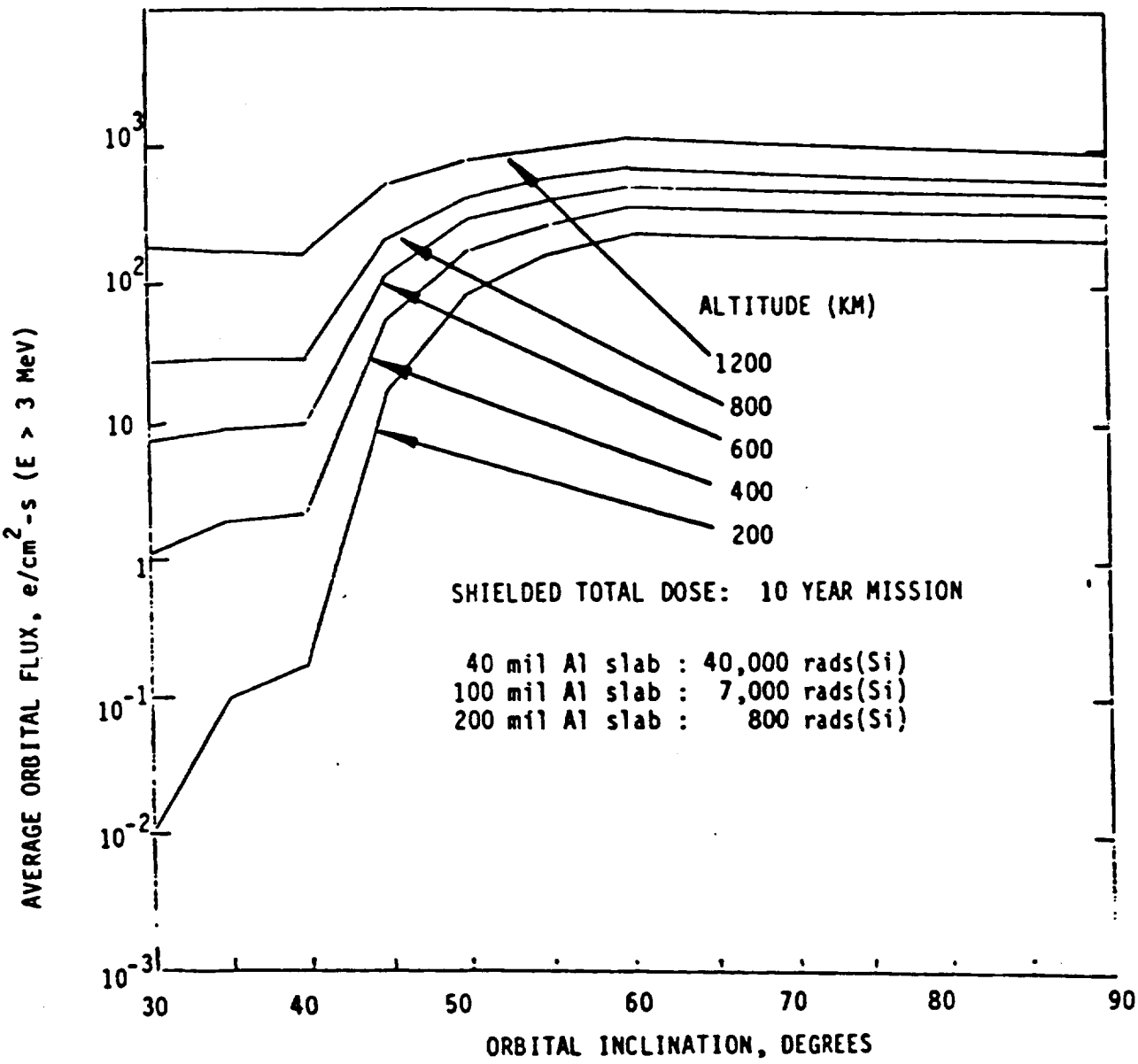

Fig 2.5.1-1 Terrestrial high energy electron environment (from E.G. Stassinopolus, Ref. 3).

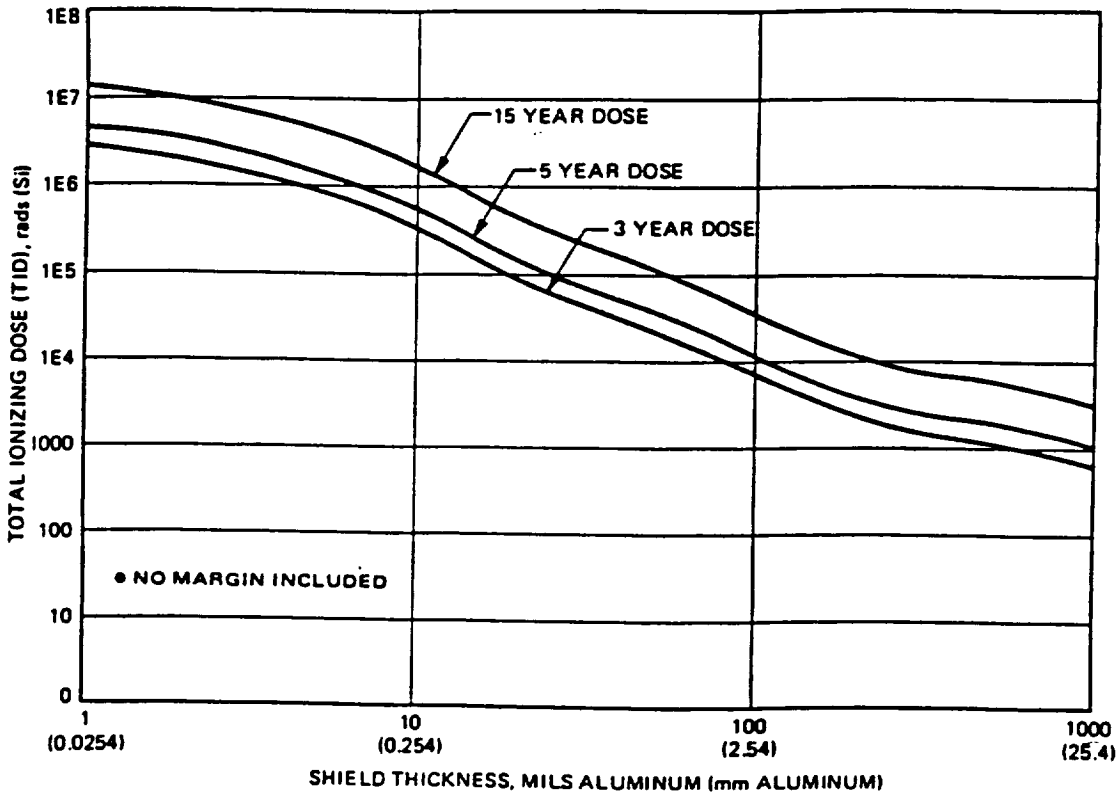

Fig 2.5.1-2 **Total Ionizing Dose Levels for 824 km Polar Orbit**

Problem areas remaining are the streak tube, high voltage power supply, the CCD camera, and the high voltage sweep drivers. CCD cameras are radiation hard up to about 1krad, which is equivalent, as shown in Fig 2.5.1-1, to 0.2 in of aluminum shielding for 10 y. Replacement components and/or total circuit replacements may be required.

2.5.2. Worst-Case Estimates

Radiation produced by solar flares is so intense that any amount of shielding being considered will have negligible effect. This limit corresponds to an unshielded condition. Examples of conditions that might arise for this zero-shielding condition are false sweep generation, and logic circuit latch-up. Neither of these conditions are permanently detrimental to the operation of the streak camera.

2.5.3. Other Radiation Effects

Browning of the fiberoptic input and output windows in the streak tube is one concern. The cathode, the metal/ceramic body, the metal electrodes, the MCP, if one is used, and the phosphor screen components in the streak tube are not known to be susceptible to permanent damage in the radiation environment.

High energy induced scintillations within the input window that are coupled to the cathode, or within the phosphor screen/output window assembly, can cause spurious noise pulses and/or a reduction in the signal/noise ratio. However, the expected event rates are much too low to be of concern for the streak camera. Spurious pulses due to ionizing radiation interactions within the CMCP, phosphor screen and SSA readout assembly are also possible. None of these effects are considered serious because of the short gated-on times for the streak tube. Additional suppression of spurious signals in the streak tube can be achieved by CMCP gating.

With a low noise SSA readout system cosmic ray induced events are easy to identify, and they can be eliminated during signal processing of the data. The pervasive cosmic rays can induce signals from the input window, cathode, MCP, phosphor screen, coupling windows, and SSA readout device. It is Laboratory for Laser Energetics' experience, with ground based laboratory streak tube systems, that about 1 significant cosmic ray event is recorded in every 10 readout frames. Since the cosmic ray flux is not significantly higher in orbit, shielding against this component of the background radiation is not recommended. With any spacecraft camera, it is advisable to provide for flat-field background subtraction of fixed pattern noise.

It is recommended that a magnetic shield be part of the potted streak tube assembly. This is a convenient and effective way to protect the linear deflection in the streak tube from unwanted and spurious deflections from magnetic fields generated in surrounding equipment. An example of a streak tube in a high voltage potted assembly with flying leads and a magnetic shield is the ITT #F4157 streak tube shown in Fig 1.1-4. This figure also shows the two mounting rings, which provide accurate and sturdy alignment of the streak tube in its mechanical holder, at the ends of the streak tube assembly.

2.6. Lifetime

Hamamatsu Corp[30] has been asked to comment about the requirement 1E9 deflection reliability streak cameras. Although this figure is believed to be achievable, by using a proprietary method of aging and selecting avalanche transistors, they are not able to guarantee at this time that the 1E9 deflection requirement over a 5 y period can be met in the space qualified streak camera.

In order to determine streak camera lifetime, ie MTBF, a component list with the known or estimated stress present on each part is needed. ITT/ACD has estimated about 10 h over a 1 w period to review a streak camera parts list alone. This task does not include lifetime estimates. For complete backup data and estimates, the task involves a look at familiar circuit cards and the unfamiliar tube assembly,

high voltage power supply, and deflection drive. Assuming replacement parts will be found for the three unfamiliar assemblies, the MTBF could be estimated with about 6 x 40 + 3 x 40 = 360 h of reliability engineering.

2.6.1. Streak Tube Lifetime

By making some reasonable assumptions the lifetime of the streak tube can be estimated. For example, assuming that the cathode will loose half its sensitivity at 532 nm after emission of a charge density of $1C/cm^2$, if 1E9 pulses are detected, and if 100 e are emitted in each pulse from cathode spot diameter of 100 μm, ie a cathode area of $8E3\ \mu m^2 = 8E\text{-}5\ cm^2$, the total estimated emitted charge density is $1E9 \times 100e \times (1.6E\text{-}19C/e)/8E\text{-}5\ cm^2 = 2E\text{-}5C/cm^2$. This is five orders-of-magnitude less than the half-life charge density[31], so the cathode life is estimated to be a negligible problem for this application, especially if the streak tube is properly gettered, electron scrubbed, if a remote-process photocathode with a conductive underlay is used, and if operation in maintained away from the ion-burn-spot area at the center of the photocathode. The phosphor screen in the streak tube is also robust, and it will not present a life problem for this application. The International Ultraviolet Explorer (IUE) tubes, with their Cs-Te cathodes and KA (P20) phosphor screens, have been shown to be very reliable in a space instrument application.

2.6.2. Cascade Avalanche Transistor Drive Circuits

The main life limiting component in a linear scan streak camera is the deflection drive circuit. A sample sweep generator, or deflection drive, circuit is shown in Fig 2.6.3-1. Transistors operated in the avalanche mode[32], avalanche transistors, are used in in the deflection circuits of almost all streak cameras, but they are considered to be a major life factor for the space qualified streak camera. For example, manufacturers of avalanche transistors typically do not sell them to a specification. The user must purchase a large quantity of avalanche transistors and then proceed

to burn-in and select useable ones. For laboratory streak cameras literally thousands of avalanche transistors are burned-in and tested before enough are qualified for use in the deflection circuit. Typical types of rf power transistors used in the avalanche mode are #2N3700 and 2N5551. During operation, if one avalanche transistor fails it produces an excessive voltage on the remaining avalanche transistors in the series string of avalanche transistors, and the net result is a failure of the whole string! In order to make this string of avalanche transistors reliable, additional circuit and/or component changes need to be made.

It has been found by LLE[33], LLNL, and other users that the required cascade string of avalanche transistors have a high failure rate. Although this not a well published fact, it is common experience with streak camera users and developers.

S Thomas, et al, [34]have studied the stability characteristics of avalanche transistors in detail. A simplified block diagram of the sweep circuit, a typical sweep waveform, and an equivalent sweep circuit for the streak camera are given in Figs 2.6.3-2 to 2.6.3-4, respectively. Type 2N3700 and 2N5551 transistors have been used for several years for streak tube drive circuits. It is found that there is a large variation in the avalanche transistor characteristics of these units from the various manufacturers. National Semiconductor transistors, type 2N3700, when operated in the avalanche mode, are found to be much more stable and produce higher acceptance yield than others. This is thought to be the result of differences in the manufacturing procedures used. Small operating differences that occur in normal transistor operation can be much more pronounced in the avalanche mode. Small amounts of residual impurities, left from chemical processing, present on the junction surface area can migrate due to the high electric field at the collector/base region, causing the avalanche voltage to increase and the units become more stable. Raytheon uses a base metallization on the surface which reduces surface field effects, and their units are very stable.

These authors stablize the transistors with a power burn-in, using about 60-100 μA current for a period of about 1 mo. Recently, Raytheon types RS3500 (TO-5 can), RS3944 (TO-18 can), and RS3800 (TO-18 can), and Farranti/Plessey types ZTX300 and ZTX415 have become available, and they should be considered as good candidates for future drivers. The ZTX415 can be purchased as an avalanche transistor to avalanche transistor specifications, probably the only such unit available! In addition to the long-term burnin and selection of avalanche transistors, these authors increased the number of avalanche transistors in the string and raised the Q of the resonant circuit to improve sweep uniformity by a factor of about 2x. They give design equations for component specification, they used fast-recovery diodes to prevent undershoot and to keep the beam out of the intensifier field of view until after the intensifier is gated off, and they extended the sweep time range to over 100ns.

Follow-on avalanche transistor work is the key to the successful use of these components in the streak camera, and this work is proposed in Section 6.

2.6.3. Alternative Deflection Drive Circuits

Triode vacuum tube deflection drivers have also been considered. It is estimated that the triode cathode heater power alone will be 20W for each tube.

Another possibility is to use a meander-line deflection system driven by a single avalanche transistor. (Meander-line deflection in streak tubes has been demonstrated, possibly at the Imperial College, London, but no published reference could be found.) Its deflection sensitivity is much greater than a conventional set of deflection plates, and full screen deflection can be achieved with a drive voltage of only 300-500V. This is about 10x less drive voltage than conventional deflection, and this voltage swing can be produced by a single avalanche transistor which is much more reliable than 8-12 avalanche transistors connected in cascade. Although this has been unofficially demonstrated in the laboratory, we are not aware of

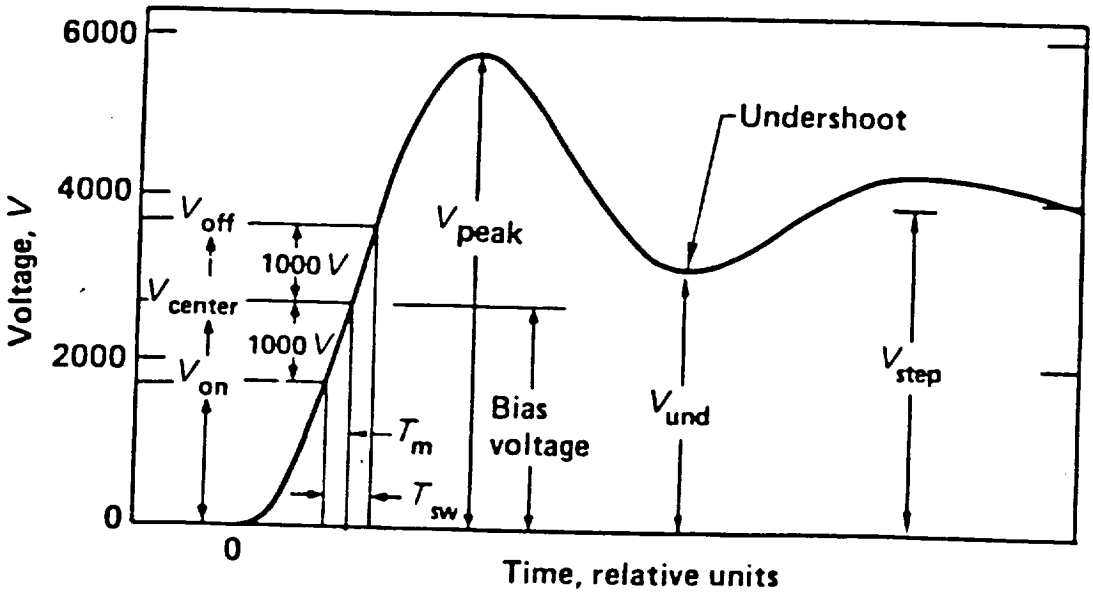

Fig 2.6.3-3 **Sweep waveform.**

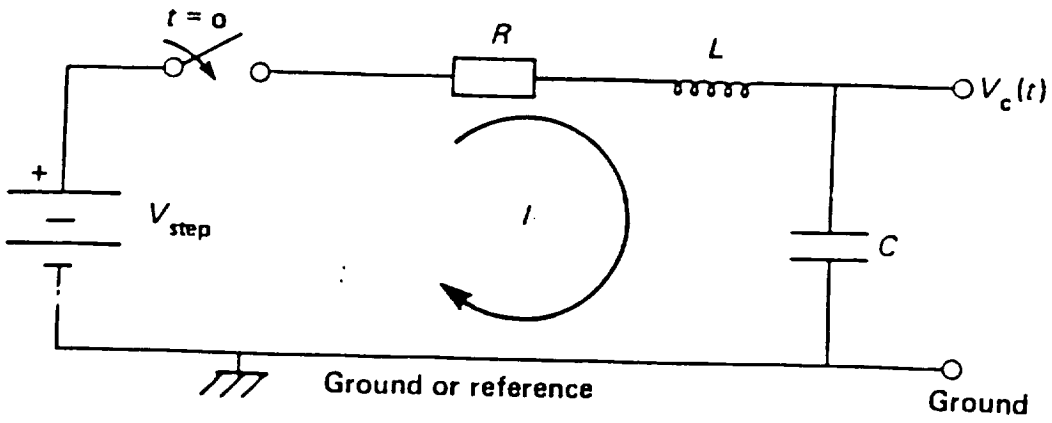

Fig 2.6.3-4 **Equivalent sweep circuit for the streak camera.**

published work in this area. Another advantage is that several of these single avalanche transistor deflection drivers could be incorporated in the streak camera and "switched" into place if necessary, thus providing backup for possible avalanche transistor failures. Disadvantages of the meander-line are that it is inherently longer than conventional deflection plates, which causes a slightly lower limiting temporal resolution, and it has not yet been fully developed for use in streak tubes.

Finally, any possibility of using redundant components in the deflection circuit needs to be considered during follow-on streak camera work, as indicated in Section 6.

2.7. Trigger Delay and Jitter

Jitter is a non-issue in the time differential mode that is now being planned for GLRS. The primary cause of a 20-30 ns trigger delay and trigger jitter in line-scan commercial streak cameras is due to the statistical variance in the turn-on characteristics of the avalanche transistor which initiates breakdown of the avalanche transistor chains. ITT/Aerospace Communications Division presently has systems limited to 1ns jitter. Commercial streak cameras, eg the HPSC FESCA-500, has a trigger delay of 20 ns at the fastest streak speed and a trigger jitter of 120 ps.

Total trigger delay consists of three components. One is due to the response time of high voltage switching transistors which serve to amplify a weak (1 V) diode signal and to protect the same diode from potentially large (200 V) back pulses from the kilovolt transients generated for the ramp. Another results from the ramp voltage waveform that can be characterized by a nonlinear knee, the linear portion used for deflection, and a final nonlinear shoulder, with approximately equal time periods in each portion of the waveform. At

the fastest streak speeds the delay should be 4 ns for the protection transistor, plus 4 ns for the first avalanche transistor, plus 1ns for the knee, minus 3 ns for the photoelectron transit time from the

cathode to the deflection plates, or 6 ns total. Slower streak speeds will have longer delays resulting from longer integration times.

Laser triggered semiconductor switches have demonstrated less than 1ps jitter, but only for very reproducible laser pulses. The time integral of the absorbed laser energy is the crucial factor for these devices.

2.8. High Voltage Power Supplies

Two manufacturers of high voltage power supplies for space qualified streak cameras have been identified. Using the voltage requirements of the ITT/EOPD streak tube #F4157 as a tentative set of specifications, summarized in Table 2.8-1, and after reviewing responses from high voltage power supply suppliers, the following comments are made.

TABLE 2.8-1 APPROXIMATE REQUIREMENTS FOR A SPACE QUALIFIED STREAK TUBE HIGH VOLTAGE POWER SUPPLY

INPUT VOLTAGE:	2816 V
OUTPUT VOLTAGES: GATED-ON OPERATION	
K	-16.50 kV
G1	-16.33 kV
G2	-16.03 kV
G3	-13.63 kV
S	0 V
OUTPUT VOLTAGES: GATED-OFF OPERATION	
K	-16.50 kV
G1	-16.56 kV
G2, G3, S	SAME AS ABOVE
HIGH VOLTAGE POTTING MATERIAL:	CONAP EN-11, OR EQUIVALENT
HIGH VOLTAGE FLYING LEADS/CONNECTORS:	REYNOLDS INC, OR EQUIVALENT

The high voltage power supply will have high voltage insulated and shielded leads extending between it and the streak tube, with high voltage connectors at the streak tube and/or the high voltage power supply.

There are two high voltage problem areas; the -16.5 kV high voltage power supply, used to provide the proper bias voltages to the streak tube, and the 12200 V deflection drivers. A high voltage power supply made by Venus and used for years by Drs Letzring and Jaanimagi at the LLE has an approximate 23,500 hr mean time to failure at +71°C. Dr Jaanimagi has found them to be very reliable, but this is not

reliable enough for the intended 5 y GLRS mission. Since capacitor life normally drops to half for each 15°C temperature rise, the Venus package may be good for more than 50 kh at a normal 23°C operating temperature. However, a thorough analysis entails a review of the MTBFs of the individual parts used in the high voltage power supply.

The 12200 V horizontal drive circuit is the absolute worst and least predictable. Deflection plates are charged to +2200 Vdc and -2200 Vdc. A series string of 20 2N3700 or similar "selected" avalanche transistors are connected between the deflection plates, with approximately 220 V across each avalanche transistor, and with all of the avalanche transistors in the "off" condition. However, since the breakdown voltage is approximately 250 V, the avalanche transistors inherently operate in a near-breakdown condition between deflection periods. An overvoltage pulse to one of the 20 avalanche transistors causes it to break-down, which causes the voltage drop across it to be reduced to essentially zero, and the remainder of the string is thereby overvoltaged, causing the entire string to become essentially shorted. The remaining 19 avalanche transistors share the 4400 V, ie 232 V each, where the weakest avalanche transistor breaks-down, and the process continues until all of the avalanche transistors break-down. In this way the voltage across the deflection plates drops to zero causing the electric field in the deflection region of the streak tube to be reversed, which in turn causes any electrons flowing through the deflection plate assembly at the time to be

deflected across the phosphor screen. To reset for the next sweep the avalanche transistors are turned off by removing their collector source voltages. The life of the circuit, as attested to by LLE, is probably about tens of hours at a repetition rate of 1 kHz. Their laboratory streak cameras contain avalanche transistors in sockets for changing all 20 with each failure.

Solutions to these problems will be difficult to find and time consuming. An analysis of additional questions, beyond the scope of this study, should also be made, eg

Is there a more suitable semiconductor device?
Will voltage equalizing resistors, capacitors and diodes improve reliability? Probably not.
What is the MTBF of the avalanche transistors?
How critical are the temperature effects on collector breakdown points?
Is radiation dose at the junctions important?
How can the radiation dose to these 20 junctions be efficiently reduced?
What is the relationship between radiation dose and the resulting avalanche breakdown threshold point?

2.8.1. High Voltage Connectors

It is recommended that high voltage connectors be used that are compatible with a high voltage rated shielded cable, such as Reynold's leads and connectors.

2.8.2. Unbalanced Deflection Driver Effects

The question here is what happens, for example, if the normal 12200 V deflection voltages become unbalanced, eg +2200 V and -2000 V? This type of problem will be corrected during the periodic recalibrations of the streak camera. On-board monitoring and downlink of all of the streak tube electrode voltages is recommended for checking the operational conditions between calibrations.

2.8.3. Streak Tube Gating

Some additional comments can be made concerning streak tube gating. Table 2.4.2-1 lists the operational high voltage power supply specifications for a slow-speed streak tube, eg the ITT F4157U. For the more demanding higher speed, ie 2 ps resolution, GLRS streak tube, higher photocathode-to-G1 voltage is required, ie at least 1 kV. No new power supply development is required to produce a 1 kV gate pulse. If a sufficiently high electric field at the photocathode cannot be achieved using a 1 kV photocathode-to-G1 potential, ie if the streak tube design will not allow a short enough photocathode-to-G1 spacing, then some high voltage power supply development will be required to provide a photocathode-to-G1 potential in the 1-3 kV range.

Electronic gating can also be achieved by gating the voltage across the CMCP used inside the streak tube. This gate voltage can be smaller than the 3 kV required at the photocathode-to-G1 gap because of the strong dependence of CMCP gain on voltage.

3. INPUT COUPLING OPTICS

The size and design of the optical inputs largely determine the size of the photocathode. Our primary recommendation to use an array of separate fiber cables to couple the output of the optical receiver to the streak camera input. This type of input coupling optic is shown schematically in Fig 3-1. The uv and green wavelengths are switched into one end of a pair of fiberoptic cables, and the signal pulses are coupled into a fiberoptic input window on the streak tube. These fiberoptic cables can be bonded to the streak tube's input window using an optical cement, or a coupling assembly can be made to hold the fibers in good optical contact with the streak tube's input window. A close-packed hexagonal arrangement of optical input fibers can be used for maximum use of the active photocathode area in the streak tube, as shown in Fig 3-2.

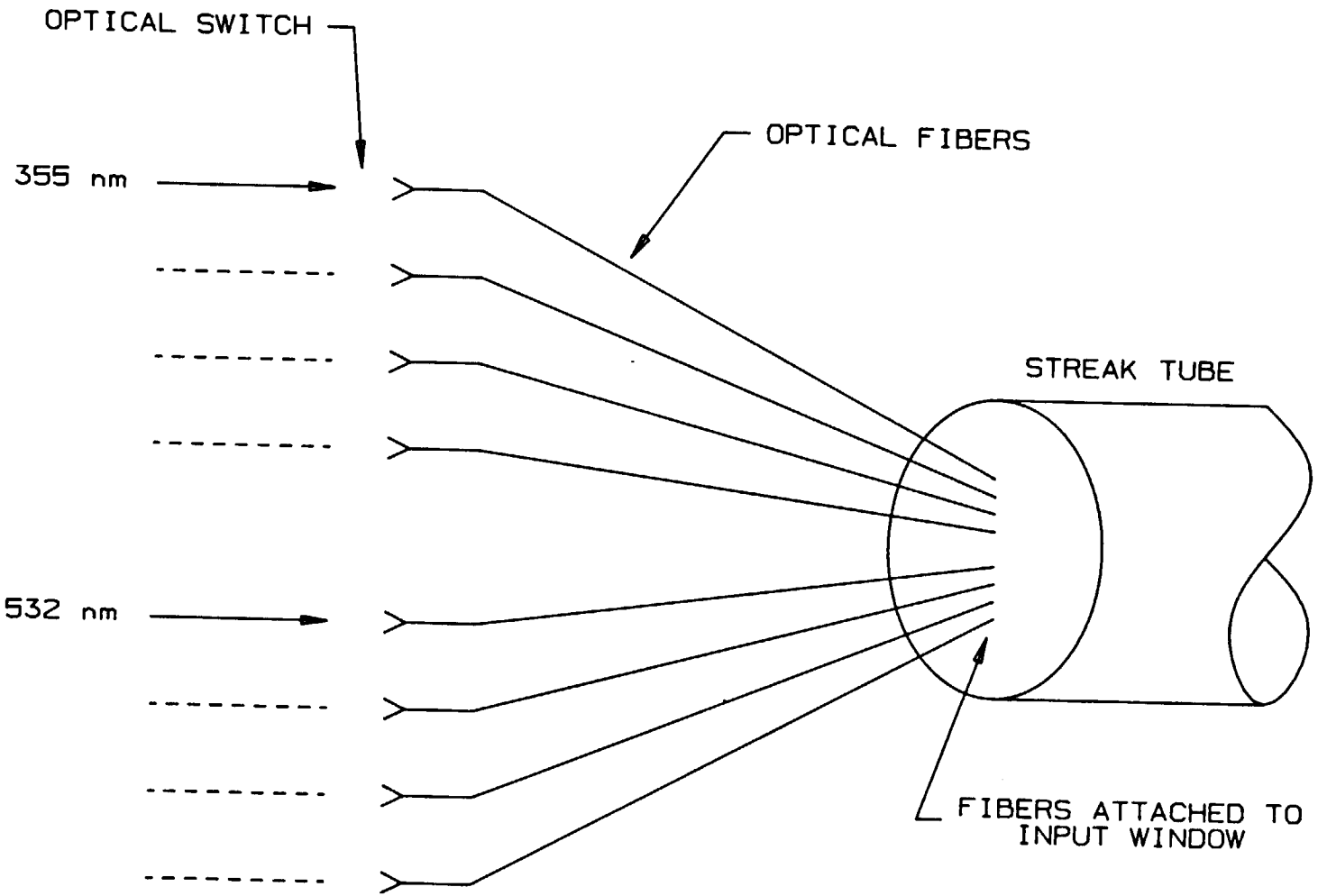

Fig 3-1 OPTICAL FIBER INPUT SWITCHING

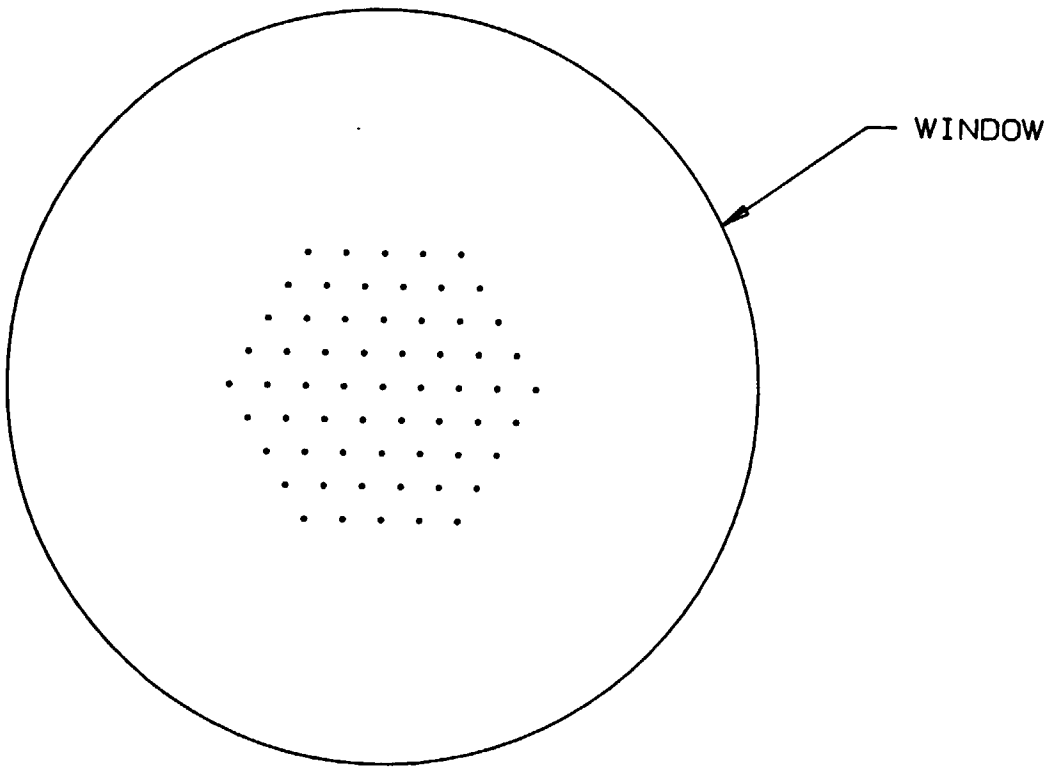

Fig 3-2 FIBER PATTERN AT STREAK-TUBE INPUT WINDOW

It is assumed that a variable optical delay line will be incorporated into the transmitter optical path to delay the 532 nm transmitted pulse from the 355 nm transmitted pulse thus allowing the return green and uv signals from the targets to be sampled within a streak tube sweep period of 500 ps[35].

Recent papers by Ihlemann et al[36] and Duncan et al[37] discuss reportedly large group velocity dispersion produced by commercial streak camera objective lenses. The group velocity dispersion can be large and is important if simultaneous picosecond timeframe measurements are made of widely separated wavelength pulses. For example, Duncan et al[38] observed anomalous pulse advances of a 22 ps duration 683 nm pulse relative to a 532 nm pulse of the same duration.

Baseline fiberoptic input coupling parameters are given in Table 3-1.

TABLE 3-1 FIBEROPTIC INPUT COUPLING PARAMETERS

FIBER DIAMETER:	20 μm
LOW SUSCEPTABILITY TO RADIATION DAMAGE AND EXCITATION:	FUSED SILICA
INDEX OF REFRACTION: (N = 1.45 FOR FUSED SILICA)	N
FIBEROPTIC LENGTH:	L
OPTICAL DELAY: (c = 3.00E8 m/s)	NL/c, s
OPTICAL DELAY PER METER:	3.33N, ns/m
LOSS ESTIMATE: (AT 355 nm)	0.065dB/m

The resultant temporal resolution limit (tr) of the streak camera as a function of fiber diameter (w) is given by

$$tr = \sqrt{((w/vs)2 + (dv/(\mu E))2 + 1/(vs\ fl)2)}, \qquad (3\text{-}1)$$

where vs is the streak velocity at the phosphor screen, dv in the spread in electron emission velocities at the cathode, u is the electron charge/mass ratio, ie 1.76E11C/kg, E is the electric field

strength at the cathode surface, and fl is the limiting spatial resolution at the phosphor screen. For the limiting case in which the resolution is limited only by the fiberoptic,

$$tr = w/vs, \qquad (3\text{-}2)$$

and if w = 20 μm and vs = 20 mm/ns, then tr = 1 ps.

Assuming that a 20 μm diameter fiberoptic is coupled to the fiberoptic input window of the streak tube containing 6 μm diameter fibers, the effective diameter of the combination is 26 μm, increasing the estimate above to 1.3 ps. Direct fiber-to-fiberoptic window is recommended because it is more reliable than lens coupling.

A scheme for optical fiber input switching is shown schematically in Fig 3-1. In this figure the fibers are firmly attached to the fiberoptic input window of the streak tube, and the two input wavelength signals are switched to two individual input fibers using an optical switch. Various types of fiberoptic couplers, that might be used in the design of the input coupling optics section, are shown in Fig 3-3.

It has been found that hydrogen treatment of optical fiber waveguides with pure silica cores and boron, fluorine co-doped silica claddings effectively reduces the gamma-ray induced loss increases in the visible wavelength spectral region[39]. Additional information on radiation effects in fiber optics is given by West[40]

A good review of the general principles that should be considered in designing an input coupling optical system to image signals from optical fibers onto the photocathode of a streak tube is given by Reedy[41].

4. STREAK-TUBE AND IMAGE INTENSIFIER TUBE

The design/performance tradeoffs of the streak-tube and the image intensifier relate directly to the overall streak camera design. For example, a demagnifying electron lens in the streak-tube requires

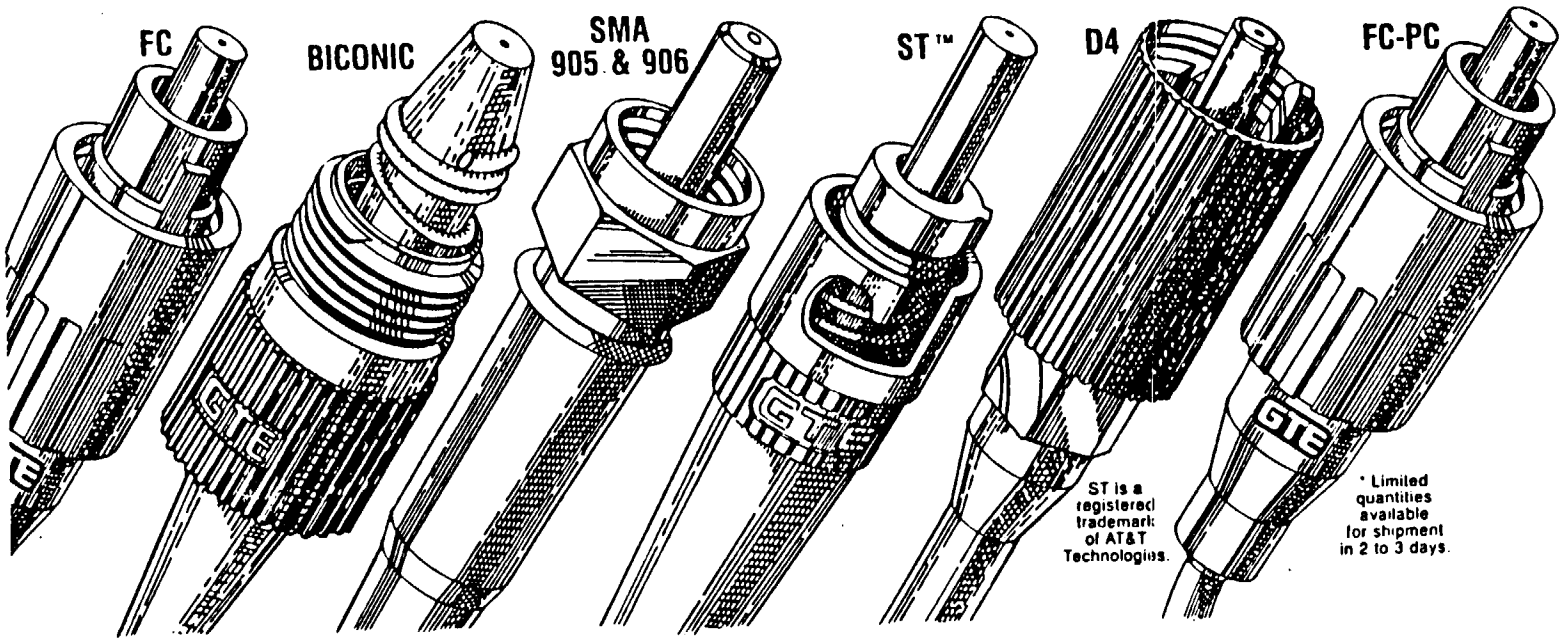

Fig 3-3 Various Types of Fiberoptic Cable Connectors

less beam deflection power, it reduces the streak-tube length, it produces more brightness gain, and it reduces the size of the output streak patterns for better, or direct coupling to an SSA: however, it requires that high resolution phosphor screens be used to preserve the image information. Other significant technical and system tradeoffs occur in choosing the type of gain mechanism: For example, an MCP can be used inside the streak-tube so that a separate image tube is not needed, or an MCP image tube with unity magnification can be coupled to the output of the streak-tube, or a demagnifying electrostatic focus image tube without an MCP can be used in its place, or etc. Each of these possibilities has a large impact on the overall streak camera design, thus several tradeoffs were considered.

Two choices of input window material, ie uv fiberoptic or fused silica, can be made for the streak tube. The optical transmissions of these materials are shown in Figs 1.2.2-1 and 4-1. Because of its higher transmission, higher effective quantum yield is possible with fused silica. The input optical interfaces will be completely different for these two materials. Since fused silica is transparent, either lens coupling, or possibly self-focusing fiberoptic cable/lens[42], is required between the optical system and the streak tube.

If a uv fiberoptic window is used, then simple direct optical coupling to input fiberoptic cables can be used. Individual fiber diameters in a uv fiberoptic window are typically 6 μm. The effective input diameter optical excitation at the cathode is a convolution of the fiberoptic cable and input window fiber diameters, or, if fused silica is used, it is the optical image spot diameter at the cathode. Some of the broader implications of the input optical coupling design are given in Section 3. Fused silica is known to be resistant to possible radiation "browning[43],[44],[45]," but no information on this subject has been found for uv fiberoptic windows.

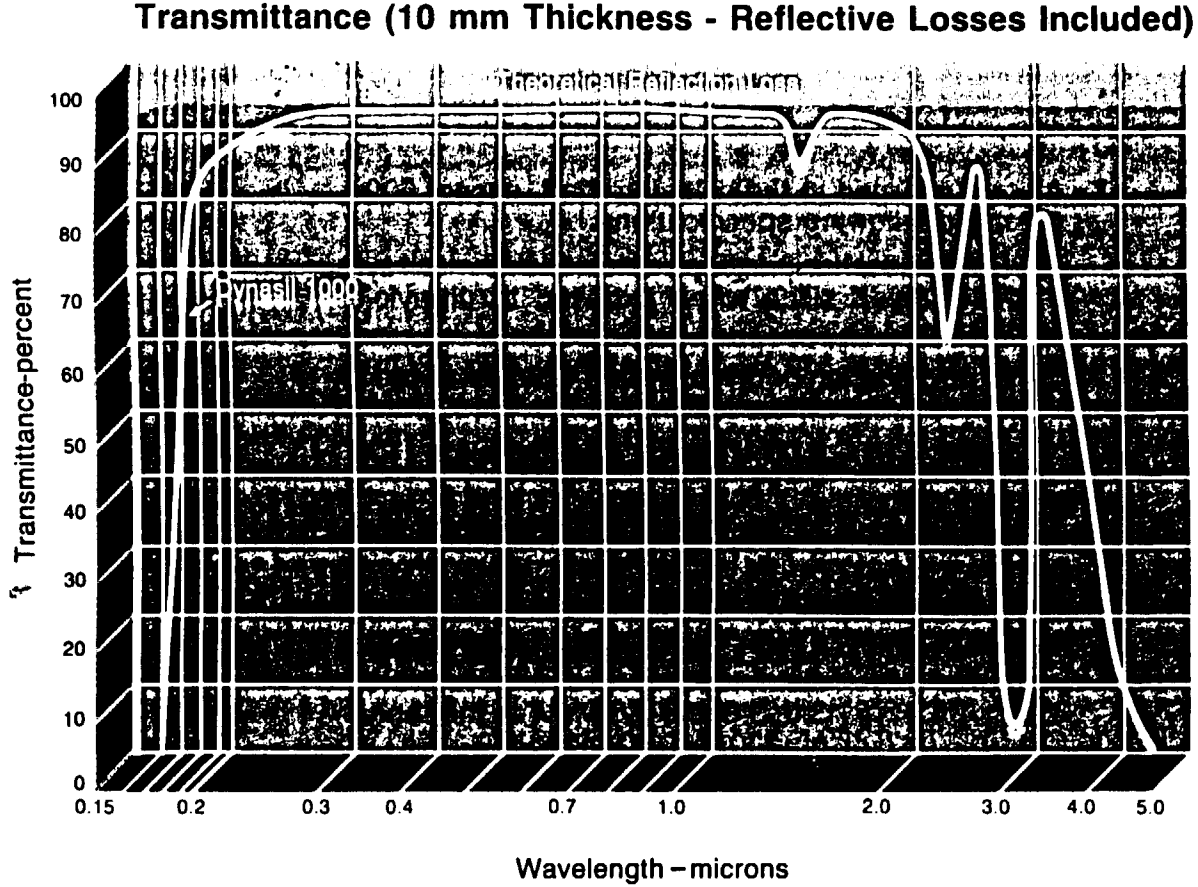

Note: Above transmittance curve is typical of stock materials.

Fig 4-1 Dynasil-1000 Fused Silica Optical Transmission vs wavelength

The performance characteristics of a streak tube having an internal MCP have been described by Sibbett, et al[46]. Resolutions of 1ps and 4ps were achieved in the synchroscan and single-shot modes, respectively.

It is recommended that the streak tube design, as shown schematically in Fig 1.1-3, be used for the GLRS streak camera. This design employs a high gain and high resolution microchannel plate, eg a CMCP, which provides for single photoelectron sensitivity, and it eliminates the need for an external image intensifier tube.

A small streak tube needs to be seriously considered during follow-on work, because it can affect several streak camera characteristics. A smaller streak tube output matches better to the available size of SSAs, lower deflection voltage can be used, and the use of high frequency switching MOSFETS becomes a possibility. This line of attack needs to be further explored, and is contained the streak-tube design follow-on task in Section 6.

5. OUTPUT OPTICS AND READOUT OPTICS

A practical way to couple the output optical streak pattern form the streak tube into an SSA chip is to use a fiberoptic taper. For example, in order to couple the light pattern from a 40 mm diameter streak tube output fiberoptic window into an 11-16 mm diagonal SSA taper, as shown schematically in Fig 5-1, could be used. The 16mm diagonal is large enough to allow the use of a dual linear solid state Reticon type #RL-512 array, having 512 25 µm wide by 2500 µm long pixels in each array. Alternatively, an area SSA, eg a Thomson-CSF charge-coupled device, can be used. Figure 5-2 shows the layout of both a dual linear array and an area SSA within the 16mm diagonal, and Tables 5-1 and 2 show some of the characteristics of the output optics and these two readout devices.

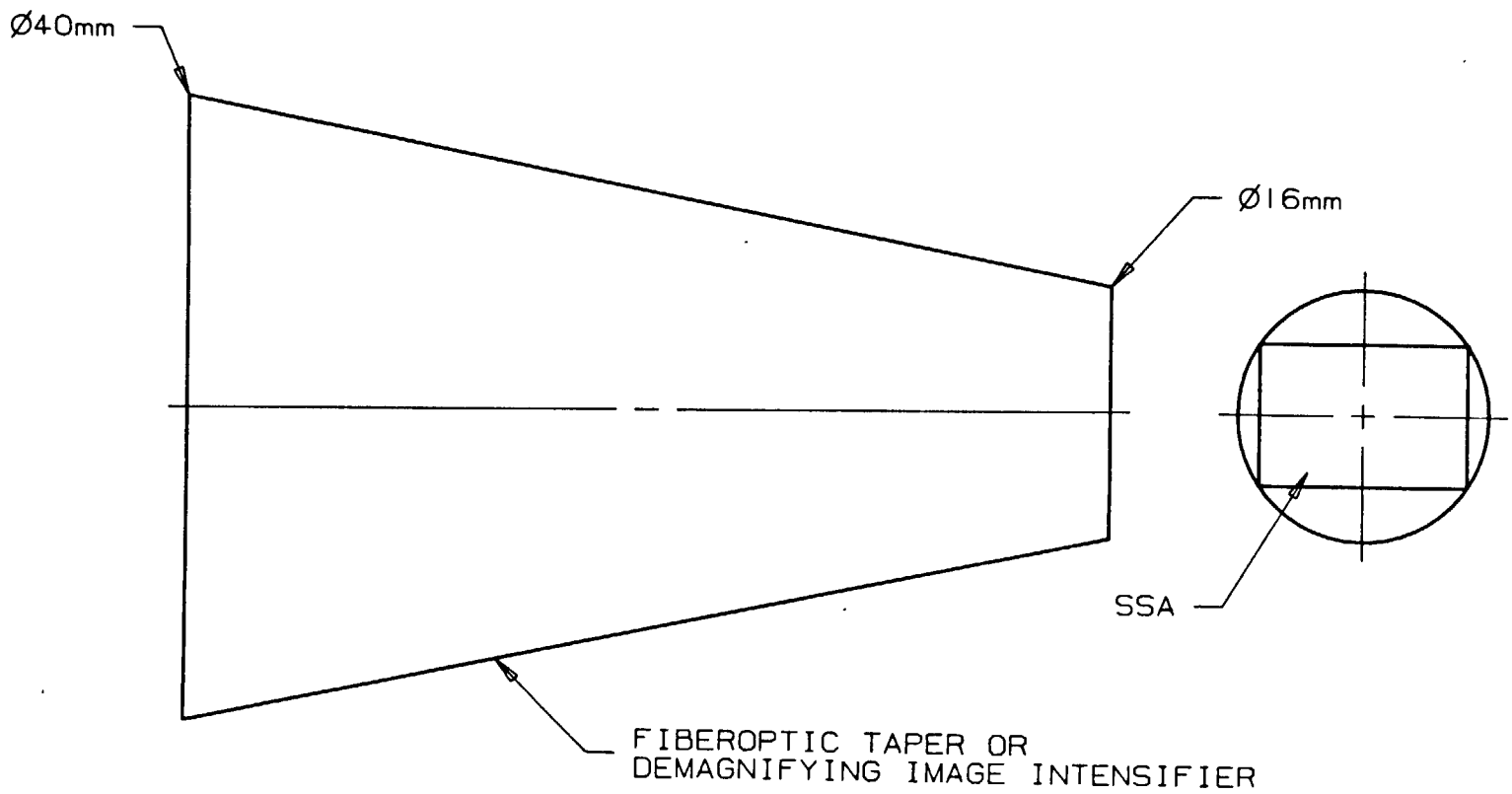

Fig 5-1 STREAK-TUBE TO SSA COUPLING

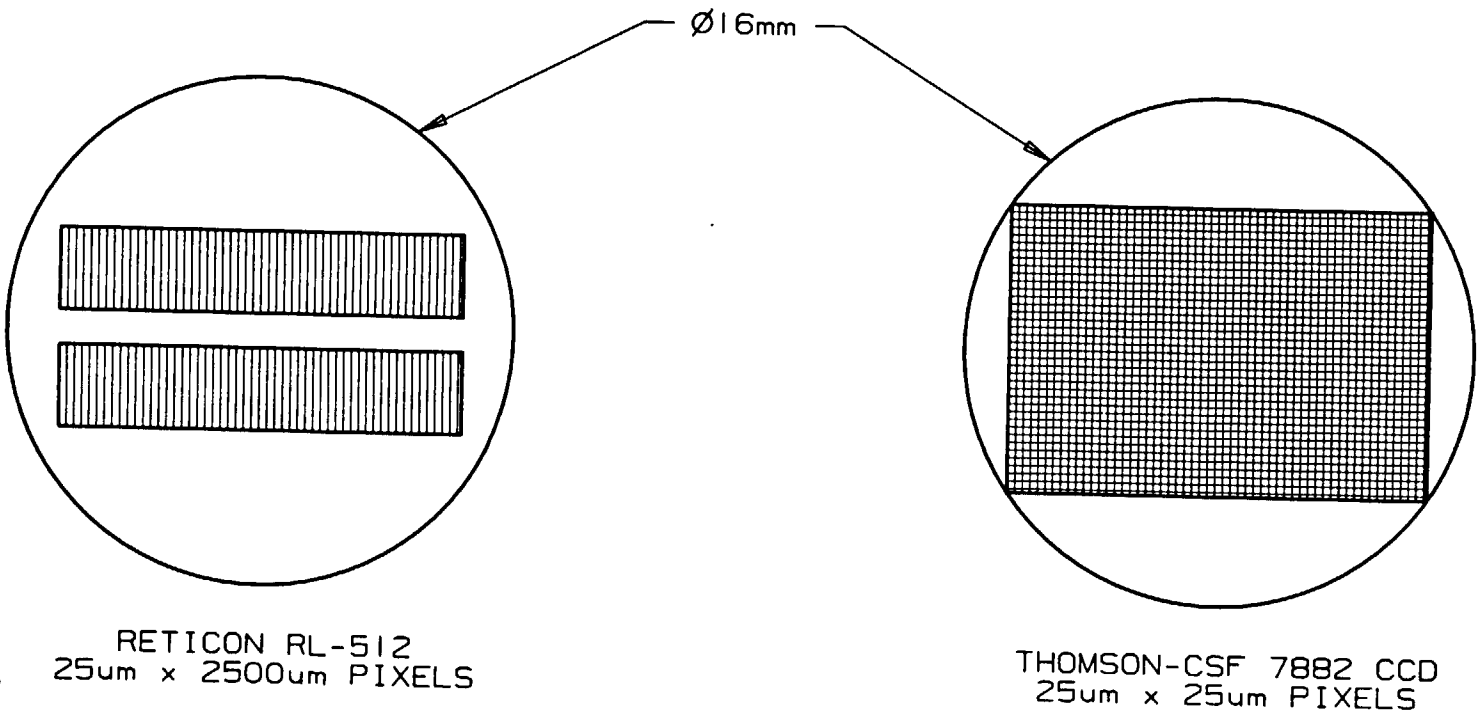

Fig 5-2 DUAL-LINEAR & AREA READOUTS

TABLE 5-1 OUTPUT OPTICS AND DUAL LINEAR RETICON ARRAY READOUT DEVICE

ARRAY LENGTH; 12.8 mm, EACH
ASSUMED STREAK TUBE OUTPUT DIAMETER; 40 mm
DATA RATE; 512 px x 40/s x 8 bit/px = 160 kbit, each array
DIAGONAL OF DUAL LINEAR 512 PIXEL ARRAY ASSEMBLY; 14.2 mm
DYNAMIC RANGE; 100,000/1
FIBEROPTIC COUPLER INPUT/OUTPUT DIAM RATIO; 40/14.2 = 2.8
MINIMUM READOUT PERIOD; 0.1 ms
NUMBER OF PIXELS; 512
OUTPUT NOISE; 1300e, rms (10ms integration time, +23°C)
PIXEL CENTER-TO-CENTER SPACING; 25 μm
SATURATION CHARGE; 14 pc

TABLE 5-2 OUTPUT OPTICS AND THOMSON-CSF CHARGE-COUPLED DEVICE READOUT

AREA SSA; THOMSON-CSF #TH7883 CCD

PIXELS; 576 X 384

PIXEL SIZE; 23 μm X 23 μm

DIAGONAL; 15.9 mm

DYNAMIC RANGE; 5000/1

OUTPUT NOISE; 28e, rms (200 kHz - 500 kHz, -45°C)

MINIMUM READOUT PERIOD; 25 ms

PIXEL READOUT; 8 bit each pixel
384 pixel/trace x 2 trace x 40/s = 30.7 k pixel/s

The requirements for single photoelectron detection using microchannel plate image intensifier tubes fiberoptically coupled to solid-state self-scanned arrays, and the signal-to-noise ratio properties of image are discussed elsewhere[47],[48]. Before making a final readout device choice the operational parameters, eg readout

noise, pixel saturation charge, etc, of the candidates, eg Reticon photodiode array, Thomson-CSF #TH7882 charge-coupled device, etc, need to be compared against the sensitivity and dynamic range requirements in particular. The general streak tube design discussed in this report, containing the high resolution CMCP, and fiberoptically coupled to a SSA readout TV camera, is capable of reaching both photoelectron counting sensitivity and the desired 2ps temporal resolution.

6. RECOMMENDED FOLLOW-ON TASKS

Considering this study to be Step I in the program to develop flight model streak cameras for GLRS, we are now in a position to make recommendations for the next step. Table 6.1 summarizes our recommended follow-on tasks for Step II. These tasks include increased focus on weak-links, exploration of candidate solutions,and breadboard tests to prove that the solutions are viable.

Results deriving from these tasks will be analyzed and discussed in reports, and specifications and designs will be proposed dealing toward Step III, which will be to develop the engineering model and acquire material for the prototype model. In Step IV the prototype will be developed, qualification tests will be performed, and long-lead items for flight model streak cameras will be ordered. The flight model streak cameras will be made in Step V.

TABLE 6.1 GLRS STREAK CAMERA STUDY RECOMMENDED FOLLOW-ON TASKS

MAJOR STUDY AREA	TASK	DURATION * (WEEK)
SIZE	ESTIMATE TUBE, CIRCUITS, AND READOUT CAMERA NEEDS	4
MASS	ESTIMATE FROM RUGGEDNESS AND RADIATION ENVIRONMENT TASK RESULTS	4
RUGGEDNESS	NASTRAN ANALYSIS OF STREAK TUBE DESIGN	16
	DETAILED CAD ANALYSIS OF POTTED AND RUGGEDIZED TUBE, HVPS, CIRCUITS ASSEMBLY	32
TEMPERATURE	CIRCUITS LIMITS	4
RADIATION ENVIRONMENT	LIMITS FOR SSA, SSA CAMERA, HVPS, DEFLECTION DRIVER	32
LIFETIME	COMPONENTS (FROM KEY PARTS LIST) MTBF ESTIMATES	36
TRIGGER DELAY	STUDY NEW TECHNOLOGY, GaAs CIRCUITS	30
HVPS CIRCUITS	STUDY AVALANCHE TRANSISTOR DEFLECTION DRIVER DESIGNS AND OPERATIONAL LIFE LIMITS	25
DESIGN	STREAK TUBE	
	- CATHODE LIFETIME	5
	- CATHODE SENSITIVITY VS RESOLUTION	10
	- SPACE CHARGE EFFECTS	5
	- EP DESIGN, CATHODE-TO-G1	26
	- SMALL DESIGN	26
	- TRAVELING-WAVE DEFLECTION WITH SINGLE TRANSISTOR DRIVER	10
	- SSA READOUT INSIDE TUBE	10
	- SYNCHROSCAN/CIRCULAR SCAN	

TABLE 6.1 (Cont'd)

MAJOR STUDY AREA	TASK	DURATION * (WEEK)
DESIGN Cont'd	STREAK CAMERA	
	- STREAK TUBE-TO-CAMERA FIBEROPTIC COUPLING	15
	- FRESNEL LOSSES AT FIBEROPTIC INPUT	15
	- DETAILED SNR ANALYSIS FOR CANDIDATE STREAK TUBE DESIGNS	30
BREADBOARDS AND TESTS	LIFETEST	
	- STREAK TUBE CATHODE	20
	- AVALANCHE TRANSISTOR CIRCUIT	40
	- HVPS (dc)	20

* NOTE: DURATION WHEN TASK DONE IN PARALLEL WITH OTHER TASKS

7. SUMMARY

A summary of this study report has been published in the literature[49].

A remotely processed dual photocathode assembly, using one photocathode for each input wavelength, is proposed as the best chance to achieve optimum temporal resolution and quantum yield results in a single streak tube. Nevertheless, at 355 nm the 2 ps resolution will be hard to achieve, because of the increased electron transit time spread, but the desired 25% quantum yield can be met. The reverse situation exists at 532 nm, ie 2 ps resolution will be easily attainable, but it will be difficult to achieve the desired 20% quantum yield. These issues are not considered to be showstoppers for the GLRS mission, but the broader system performance implications need to be reviewed. Although avalanche transistor streak camera circuits have been unreliable in the past, significant recent avalanche transistor reliability work at LLNL, and possibly within streak camera companies, may offer the required solution to this issue. With the exception of the streak camera's sweep circuit reliability question, relating to the use of avalanche transistors in particular, it is concluded that a suitable streak camera for the GLRS application can be space qualified in the Phase C/D timeframe.

8. APPENDIXES

8.1. Temporal Resolution Requirements

8.2. Streak Camera Performance Model

APPENDIX 8.1 - SPACE QUALIFIED STREAK CAMERA STUDY

1 TEMPORAL RESOLUTION REQUIREMENTS

1.1 INTRODUCTION

The initial requirements were that the streak camera should have a temporal resolution of "2_ps FWHM or better in both channels at the single photoelectron level. Not to exceed 8_ps FWHM at maximum amplitude." NASA has asked for an elaboration on how we will meet these requirements, comments on those requirements which we feel are unrealistic, and proposals for levels which we feel are more achievable.

1.2 TEMPORAL RESOLUTION LIMITS

Some initial discussion of our interpretation of the temporal resolution performance requirement is needed before we elaborate on it. It is assumed that an image intensifier tube will be required between the streak-tube and the readout camera to produce a signal spot in the camera's pixels that is well above the camera-induced pixel noise level. The individual photoelectron event light spots that appear at the phosphor screen of the image tube will expose the readout camera pixels and produce the pixel charge pattern scanned by the camera. It is assumed that the centroid of this charge pattern will be determined and stored in memory. Successive repetitive similar scans and stored centroid locations will yield a histogram of events, and this histogram will have its own peaked distribution shape. The peak of this histogram is assumed to be the event occurrence time, and its FWHM is a measure of the system noise associated with the measurements. In our analysis we will first consider the limiting temporal resolution of the optical input, streak-tube, image tube, and readout camera components, including the resolution losses resulting from the image transfers between each of these components. Then an estimate will be made for the FWHM resulting from optical input fluctuations, jitter in the gate and trigger circuits, signal-to-noise ratio in the readout, etc.

The three major limiting factors directly related to the temporal resolution of the streak-tube are the input optical "spot size" limit (ts), the electron "chromatic" transit-time spread limit (tc) due to the spread of emitted electron energies and directions, and the effective "technical" resolution limit of the streak-tube and readout assembly (tt). The details of each of these limits are discussed in the following sections.

Assumptions and definitions used for this analysis are as follows:

δv	emitted photoelectron velocity spread
δV	emitted photoelectron energy spread
u	electron charge/mass ratio
E	photocathode electric field strength
M	electron lens magnification, cathode-to-screen
vs	streak velocity at the phosphor screen
fls	limiting spatial resolution of streak-tube
W	optical input slitwidth
ts	input optical "spot size" resolution limit
tc	electron "chromatic" transit time spread resolution limit
tt	"technical" resolution of the streak tube
tr	resultant temporal resolution
Ls	streak length at phosphor screen
Vk	potential difference between cathode and G1 electrodes
Lk	distance between cathode and G1 electrode

In order to meet the temporal resolution requirements several operational parameters need to be carefully controlled. It is useful to consider a simplified physical model which highlights the key parameters. It should be emphasized that this analysis estimates the limiting temporal resolution, not the temporal resolution corresponding to the FWHM response point, so it gives optimistic values. If it is assumed that the spread functions are all gaussian, then we can adjust our calculated results by a single factor. Let the following values be chosen for the parameters defined above.

$M := 1$ $\qquad ts := 0.5\ ns$ $\qquad Ls := 20\ mm$

$$vs := \frac{Ls}{ts}$$

$$vs = 4 \cdot 10^{7} \cdot \frac{m}{s}$$

$$W := 100 \cdot \mu m$$

$$fls := \frac{12}{mm}$$

$$\delta V := .3 \cdot V$$

$$E := 1 \cdot 10^{6} \cdot \frac{V}{m}$$

The three major temporal resolution limiting components, ie the input "spot-size" limit, the electron "chromatic" limit, and the "technical" limit, are defined as follows, and these definitions are used to calculate the individual component resolutions for these assumed values.

$$ts := M \cdot \frac{W}{vs} \qquad ts = 2.5 \cdot ps$$

$$tc := \frac{\sqrt{2 \cdot \frac{\delta V}{|u|}}}{E} \qquad tc = 1.8 \cdot ps$$

$$tt := \frac{M}{vs \cdot fls} \qquad tt = 2.1 \cdot ps$$

By adding these limits in quadrature, we estimate the resultant (tr) to be

$$tr := \sqrt{\left[\frac{M^2}{vs^2}\right]\cdot\left[W^2 + \left[\frac{1}{fls^2}\right]\right] + \left[2\cdot\frac{\delta V^2}{|u|\cdot E^2}\right]} \qquad tr = 3.7\ ps$$

Under these same conditions, but with the sweep period adjustable in the 0.5-4.5_ns range, the resultant temporal resolution is found to be as follows.

$$i := 0\ ..8 \qquad ts_i := (i\cdot 0.5\ ns) + 0.5\ ns$$

$$vs_i := \frac{Ls}{ts_i}$$

$$tr_i := \sqrt{\left[\frac{M^2}{vs_i^2}\right]\cdot\left[W^2 + \left[\frac{1}{fls^2}\right]\right] + \left[2\cdot\frac{\delta V^2}{|u|\cdot E^2}\right]}$$

The streak velocity vs (m/μs), streak period ts (ns), and resultant temporal resolution tr (ps) values are given in the following table, and tr vs vs is plotted.

vs_i	ts_i	tr_i
m/μs	ns	ps
40	0.5	3.7
20	1	6.8
13.3	1.5	9.9
10	2	13.1
8	2.5	16.4
6.7	3	19.6
5.7	3.5	22.9
5	4	26.1
4.4	4.5	29.3

RESULTANT RESOLUTION, (ps)

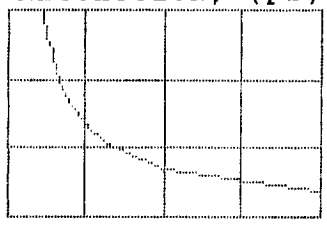

STREAK VELOCITY, (m/μs)

Thus the 2-8_ps resolution is only achieved in the 0.5~1.2_ns streak period range, which requires a very advanced deflection circuit.

For twice the limiting spatial resolution of the streak-tube, and half the optical input slitwidth

$$W := 50\ \mu m$$

$$fls := \frac{24}{mm}$$

$$tr_i := \sqrt{\left[\frac{M^2}{vs_i^2}\right] \cdot \left[W^2 + \left[\frac{1}{fls^2}\right]\right] + \left[2 \cdot \frac{\delta V}{|u| \cdot E^2}\right]}$$

vs i —— m —— μs	tr i —— ps
40	2.5
20	3.7
13.3	5.2
10	6.8
8	8.3
6.7	9.9
5.7	11.5
5	13.1
4.4	14.8

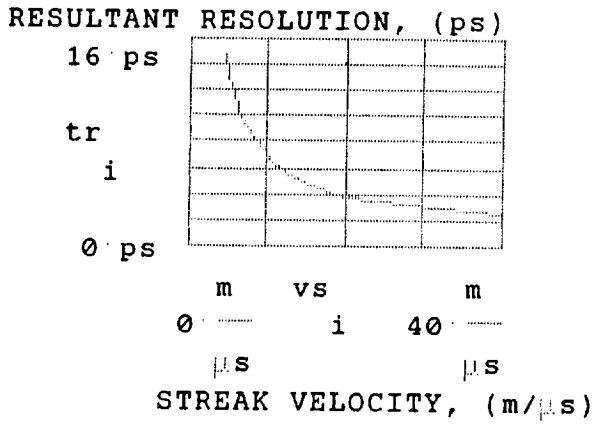

These changes clearly improve tr, but the minimum is still not 2_ps, and the deflection speed is still high. If, in addition to these changes, the cathode is chosen so that ∂V is reduced, and if the electric field strength at the cathode is increased, then the following estimates result.

$$\partial V := 0.2\ V$$

$$E := 1.5\ 10^{6}\ \frac{V}{m}$$

$$tr_i := \sqrt{\left[\left(\frac{M}{vs_i}\right)^2 \cdot \left[W^2 + \left[\frac{1}{fls^2}\right]\right]\right] + \left[2 \cdot \frac{\delta V}{|u| \cdot E}\right]^2}$$

$\frac{vs_i}{m}$	tr_i
μs	ps
40	1.9
20	3.4
13.3	5
10	6.6
8	8.2
6.7	9.8
5.7	11.4
5	13.1
4.4	14.7

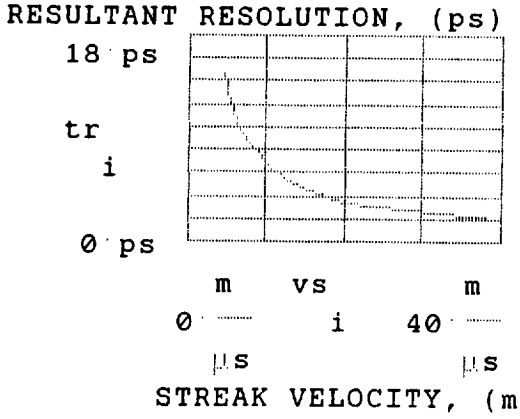

Now the limiting temporal limiting resolution, but not the FWHM, of 2_ps is just met at the highest streak velocity. Reducing the magnification in the streak-tube will reduce tr more, but then the size of the streak-tube increases, and the coupling to the camera readout must bo more carefully considered. Let us reduce M and see what happens.

$$M := 0.7$$

$$tr_i := \sqrt{\left[\frac{M^2}{vs_i^2}\right] \cdot \left[W^2 + \left[\frac{1}{fls^2}\right]\right] + \left[2 \cdot \frac{\delta V^2}{|u| \cdot E^2}\right]}$$

$\frac{vs_i}{m}$	tr_i
μs	ps
40	1.5
20	2.5
13.3	3.6
10	4.7
8	5.8
6.7	6.9
5.7	8
5	9.2
4.4	10.3

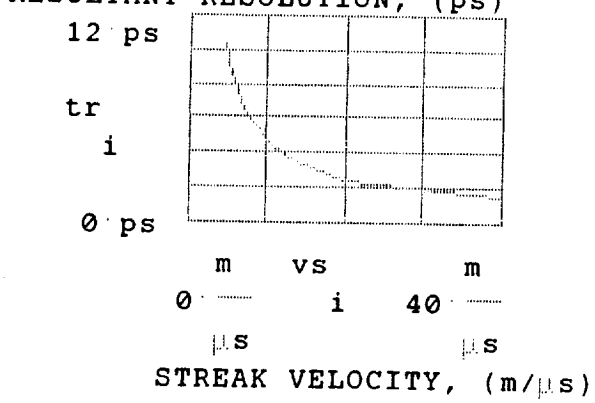

These successive changes have improved the temporal resolution, and this type of analysis should be used to design the streak tube for the GLRS streak camera system.

2 STREAK-TUBE-TO-READOUT-CAMERA CONSIDERATIONS

In order to achieve photoelectron-counting sensitivity, an image tube with sufficient gain is required between the streak-tube and the pixels in the readout camera, or preferably an MCP will be used inside the streak tube itself. The image transfer properties of this image tube, and its design, are very important to the overall performance of the system. As an initial example of the influence of this coupling on overall performance, the use of a proximity focused MCP image tube, with a limiting spatial resolution (fli) of a typical value and a magnification (Mi) of unity, will be considered.

$$fli := \frac{24}{mm}$$

$$Mi := 1$$

The limiting spatial resolutions of the streak-tube output (flso), the image tube, and the camera (flc) must be convolved in order to find the overall limiting temporal performance of the streak-camera. Note that image transfer coupling losses, eg between the input optical fiber and the photocathode, between the streak-tube and the image tube, etc, have not yet been taken into account: This will be discussed later in the analysis.

$$flso := \frac{fls}{M} \qquad Mi := 1$$

$$flc := \frac{20}{mm}$$

$$fl := \left[\frac{1}{flso^2} + \frac{1}{fli^2} + \frac{1}{flc^2} \right]^{-0.5} \qquad fl = 14 \frac{1}{mm}$$

This increases the previous estimates to the following values. Note that the expression for tr is modified to properly include the effects introduced by the use of the image tube and the readout camera.

$$tr_i := \sqrt{\left[\frac{1}{vs_i^2}\right] \cdot \left[W^2 M^2 + \left[\frac{1}{fl^2}\right]\right] + \left[2 \cdot \frac{\delta V}{|u| \cdot E^2}\right]}$$

$\frac{vs_i}{m}$ (μs)	tr_i (ps)
40	2.2
20	4.1
13.3	6
10	8
8	10
6.7	12
5.7	13.9
5	15.9
4.4	17.9

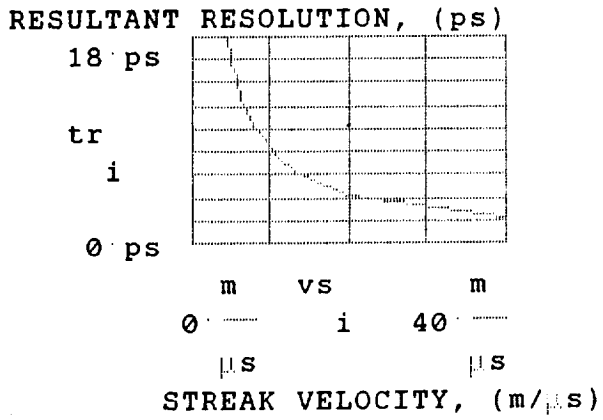

Thus the 2ps resolution is approximately reached for these assumed parameters.

APPENDIX 8.2 - STREAK CAMERA PERFORMANCE MODEL

Introduction

The performance of the streak tube is discussed in this section. Our approach to analyze the characteristics and limitations of the streak tube itself is to generally follow the paths that photons take from their time of arrival at the input window of the streak tube to the time the output trace appears at the tube's output.

Input Signal Considerations

In the photon counting limit, ie when an individual photon is detected, the passage of the photon from the source to the primary detector, eg a photocathode, is unimpeded by the intervening optical medium, and the primary detector itself responds with a quantum efficiency of 100%! This seemingly impossible occurrence is a consequence of quantum electrodynamics. For a large number of detected events the situation is much different, and we must account for the average losses and responses of the intervening optical medium and the optical detector system.

If many input photons at a given wavelength (λ) pass through the input window of the st and strike the k then an average number of photoelectrons (Y) are released. Let us make the following definitions:

- λ wavelength of input photons
- Noi number of optical input photons within an exposure period
- Yk cathode photon-to-photoelectron yield ratio (e/photon)
- Y quantum yield of input window and cathode
- Twi input optical window transmission, including reflection loss
- Sk cathode sensitivity (mA/W)

The quantum yield of the st is given by

$$Y := \left[h \cdot \frac{c}{\lambda} \right] \cdot \frac{Twi \cdot Sk}{e} \quad \square$$

where Y is in units of electrons per photon at wavelength λ, h is Planck's constant, c is the velocity of light, and e is the electronic charge. Since the absolute spectral sensitivity (S) of a st is usually a measured characteristic, we will set

$$S := Twi \cdot Sk \quad \square$$

The relationship for Y can be rewritten in simpler form as

$$Y := 124 \cdot \frac{S}{\lambda} \quad \square$$

where Y is in units of percent for S and λ in units of mA/W and nm, respectively.

The average photon arrival rate (Ipi, photon/s) at a given point is

$$Ipi := Poi \cdot \frac{\lambda}{h \cdot c} \quad \square$$

where Poi is the optical power at the point, and the corresponding pe emission rate is

$$Iek := Ipi \cdot Y \quad \square$$

$$Iek := Poi \cdot \frac{Twi \cdot Sk}{e} \quad \square$$

Optical Input Temporal Resolution

The optical input temporal resolution component (To) is determined by the input optical slitwidth (W), the magnification of the st electron lens (Ms) from the cathode to the output phosphor screen, and the streak velocity (vs) at the output phosphor screen. The relationship for To is

$$To := Ms \cdot \frac{W}{vs} \quad \square$$

For the following values

$$Ms := 1$$

$$W := 6 \cdot \mu m$$

$$Dwoa := 40 \cdot mm$$

$$Tp := 1 \cdot ns$$

$$vs := \frac{Dwoa}{Tp}$$

$$vs = 4 \cdot 10^{7} \cdot \frac{m}{s}$$

To is found to be

$$To := Ms \cdot \frac{W}{vs}$$

$$To = 2 \cdot 10^{-1} \cdot ps$$

Chromatic Time Resolution Estimate

Photoelectrons are emitted from the k with a distribution of energies in all directions from the source point in the k, but the maximum emission energy (Vek) is given by

$$Vek := \frac{h \cdot \frac{c}{\lambda} - Qe \cdot Va}{Qa} \quad \square$$

where Va is the electron affinity.

The temporal chromatic resolution limit (Tc) imposed by the electron emission distributions at the cathode itself is

$$Tc := \frac{\delta v}{u \cdot Ek}$$

$$\delta v := \sqrt{2 \cdot u \cdot Vek}$$

where δv is the spread in emission energies, u is the electron charge-to-mass ratio, Vek is the electron emission energy at the cathode, and Ek is the electric field at the cathode surface.

The magnitude of the electric field at the cathode surface is simply the ratio of the extraction electrode potential (V1) to the distance between this electrode and the cathode (L1),

$$Ek := \frac{V1}{L1}$$

For example, if we let

$$\lambda := 355 \cdot nm$$

$$V1 := 1000 \cdot V$$

$$L1 := 1 \cdot mm$$

$$Va := 2.5 \cdot V$$

then the maximum photoelectron emission energy is estimated to be

$$Vek := \frac{h \cdot \frac{c}{\lambda} - Qe \cdot Va}{Qe}$$

$$Vek = 1 \cdot V$$

and the electric field at the cathode is

$$Ek := \frac{V1}{L1}$$

$$Ek = 1 \cdot 10^{6} \cdot \frac{V}{m}$$

For the values chosen, the maximum spread in photoelectron velocity at the cathode is

$$\delta v := \sqrt{2 \cdot u \cdot Vek}$$

$$\delta v = 6 \cdot 10^{5} \cdot \frac{m}{s}$$

and the corresponding chromatic time resolution component is

$$Tc := \frac{\delta v}{u \cdot Ek}$$

$$Tc = 3 \cdot ps$$

Technical Time Resolution

The technical time resolution component (Tt) depends upon the magnification of the st electron optic (Ms), the speed of the deflected electron beamtrace at the phosphor screen output of the st (vs), and the limiting spatial resolution (Fs) of the st:

$$Tt := \frac{Ms}{vs \cdot Fs}$$

For

$$Fs := \frac{20}{mm}$$

and the previously used values, it is found that

$$Tt := \frac{Ms}{vs \cdot Fs}$$

$$Tt = 1 \cdot ps$$

Camera Readout Temporal Resolution

The temporal resolution component associated with the self-scanned array (SSA) in the TV camera readout of the st is determined by the magnification in the readout section (Mr), ie from the phosphor screen to the SSA, the Nyquist limiting spatial resolution of the SSA (Fla), and the streak velocity at the phosphor screen:

$$Tr := \frac{Mr}{vs \cdot Fla}$$

For the following pixel center-to-center spacing in the SSA (La) and magnification

$$La := 20 \cdot \mu m$$

$$Fla := \frac{1}{2 \cdot La}$$

$$Mr := 2$$

the camera readout limiting resolution component is

$$Tr := \frac{Mr}{vs \cdot Fla}$$

$$Tr = 2 \cdot ps$$

Streak Camera Limiting Temporal Resolution

For the above values for the input optical, chromatic, technical and readout components, the resulting temporal resolution of the complete

camera is estimated to be

$$Tsc := \left[To^2 + Tc^2 + Tt^2 + \left(\frac{Tr}{Mr} \right)^2 \right]^{0.5}$$

$$Tsc = 4 \cdot ps$$

MCP Gain

The gain of an MCP (Gm(Vm)) depends upon the channel length to channel diameter ratio (Lc/Dc) ratio and the MCP applied potential (Vm), and a convenient expression for MCP gain is

$$Gm(Vm) := \left[\frac{Vm}{Vmo} \right]^g \quad \square$$

where Vmo depends upon the secondary emission ratio of the channel material, and g depends upon the Lc/Dc ratio. Typical values for these parameters are as follows:

TYPE	Vmo (V)	g (UNITS)	Lc/Dc (UNITS)
MCP	350	8.5	40
MCP	530	13	60
CMCP	637	17.9	100
VMCP	700	17	80
ZMCP	1050	25	120

A CMCP or a VMCP will provide sufficient gain for single photoelectron counting. Using the gain parameters for a VMCP,

$$Vmo := 700 \cdot V$$

$$go := 17$$

and

$$Vm := 700\,V, 900\,V \ldots 1500\,V$$

the gain function is seen to be

$$Gm(Vm) := \left[\frac{Vm}{Vmo}\right]^{go}$$

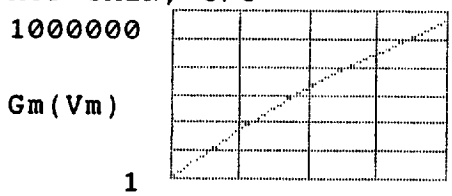

Photon Gain

The photon gain (Gp) of the st is given by

$$Gp(Vm) := \left[1.24 \cdot \frac{S}{\lambda}\right] \cdot Gm(Vm) \cdot ((Va - Vd) \cdot Ys \cdot Two) \quad \square$$

where the cathode sensitivity is given in mA/W, λ is in units of nm, Gm is the MCP gain, Va is the potential applied between the cathode and the phosphor screen, Vd is the dead-voltage of the aluminized phosphor screen assembly, Ys is the quantum yield factor of the screen assembly, ie the number of photons, with the spectral distribution of the particular phosphor, out of the screen per effective eV energy of the bombarding electrons, and Two is the optical transmission of the output window.

Some typical values can be used to estimate Gp.

$$\lambda := 355$$

$$S := 40$$

$$Va := 15\,keV$$

$$Vd := 3.5 \cdot keV$$

$$Ys := \frac{.063}{eV}$$

$$Two := 1$$

$$Vm := 1200 \cdot V$$

$$Vmo := 700 \cdot V$$

$$go := 17$$

$$Gm(Vm) = 1 \cdot 10^{4}$$

$$Gp(Vm) := \left[1.24 \cdot \frac{S}{\lambda}\right] \cdot Gm(Vm) \cdot ((Va - Vd) \cdot Ys \cdot Two)$$

$$Gp(Vm) = 1 \cdot 10^{6}$$

Thus, for this set of values, a million photons, total, emerge from the output of the tube, having the spectral distribution of the P20 phosphor. When fiberoptically coupled to a SSA camera the resulting signal in the camera can be easily detected, and photon counting operation can be achieved with the good pulse height distribution characteristics of the VMCP.

If we consider operation in the full range of applied VMCP potentials of 700-1500V, the following gain characteristic is estimated:

$$Vm := 700 \cdot V, 800 \cdot V \ldots 1500 \cdot V$$

$$Gp(Vm) := \left[1.24 \cdot \frac{S}{\lambda}\right] \cdot Gm(Vm) \cdot ((Va - Vd) \cdot Ys \cdot Two)$$

PHOTON GAIN, PHOTONS OUT/PHOTON IN

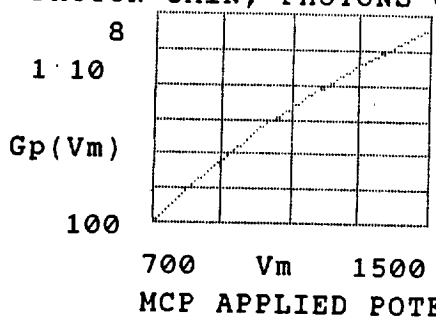

Definitions of Terms

Input Window Assembly & K-G1 Gap

Cb cathode-to-G1 capacity
Ckga total cathode-to-G1 capacity
Dkga K-G1 gap
Dip input window fiber diam
Dwim input window max od
Dwia input window active diam
Hs spherical height of input window concave surface
Rga G1 radius-of-curvature
Rwi input window radius-of-curvature
Lwia input window min thickness
Lwib input window max thickness
Lcr Cr underlayer thin-film thickness
Rk cathode resistance/square
Twi input window transmission

Electron Lens

Ra anode radius
Rs image surface radius
M electron lens magnification
N EO lens index
Va cathode-screen applied potential
Vd dead-voltage of phosphor screen assembly

Output Window Assembly

DwoM max od
Dwoa active diam
Rwo radius-of-curvature
Twoa min thickness
Twob max thickness
To temporal resolution of optical input at phosphor screen
Ms streak tube magnification, cathode-to-screen
vs streak velocity at ps
Tt technical time resolution at ps
Fs limiting spatial resolution of streak tube at ps
Fa Nyquist limiting spatial resolution of SSA at SSA
Tr temporal resolution of SSA at ps
Tsc streak camera temporal resolution
Tc chromatic time resolution
Ys quantum yield factor of phosphor assembly (photon/eV)

Two optical transmission of output window

Resolution

Feok effective resolution at cathode
Fsa resolution of screen/window assy
Fs useable resolution at tube output
Npx ssa pixels along streak line
La ssa length
Ftssa tube & ssa resolution at tube output
Fin tube input resolution for ssa readout

Tube Dimensions

LM max outside length
DwiM max outside tube diam

9. BIBLIOGRAPHY

[1] S C Cohen, et al, "The Geoscience Laser Altimetry/Ranging System," IEEE Trans Geosci Remote Sensing GE-23, 414-425(1985)

[2] J B Abshire and J E Kalshoven, Jr, "Mulitcolor Laser Altimeter for Barometric Measurements Over the Ocean - Experimental," Appl Opt 22, 2578-2585(1983)

[3] T O Edwards, Vice President, EGG Energy Measurements, Amador Valley Operations, personal communication

[4] T S Johnson, Managing Director, Hadland Photonics Limited, personal communication

[5] R Hadland, "Techniques and Applications of Image Converter Cameras," Proc 13th Int Congress High Speed Photog and Photonics, 151-161(1978)

[6] C B Johnson, et al, "Circular-Scan Streak Tube with Solid-State Readout," Appl Opt 19(20), 3491-3495(1980)

[7] W Sibbett, "Synchroscan Streak Camera Systems," Int Cong High Speed Photog and Photonics, 15-26(1982)

[8] W Sibbett and W E Sleat, "A Photochron IIC Circular-Scan Streak Camera With CCD Readout," Proc Int Cong High Speed Photog and Photonics, 543-558(1986)

[9] L W Coleman, "Ultra-Fast Streak Cameras for Laser Diagnostics," Proc Optoelectronics and Laser Tech Conf, IEEE, (1974)

[10] C B Johnson, "Photoelectronic Streak Tube Technology Review," SPIE 94, 13-18(1976)

[11] R Dupuy, et al, "Picosecond-Resolution Streak Camera and Associated Data Acquisition System," SPIE, 62-65(1976)

[12]C B Johnson, et al, "A Magnetically Focused Photoelectronic Streak Camera Tube," 12th Int Congress High Speed Photog Photonics, 56-61(1977)

[13]A J Lieber, et al, "Subpicosecond Proximity-Focused Visible Streak Camera Evaluation and Application," SPIE, 29-32(1977)

[14]S Letzring, "Buying and Using a Streak Camera," Lasers and Apps, 49-52(mar1983)

[15]P A Jaanimagi and M C Richardson, "Streak Camera for Picosecond X-Ray Diagnostics," Rev Sci Instrum 54(9), 1095-1099(1983)

[16]Y Tsuchiya, et al, "Universal Streak Camera," SPIE 491, 86-94(1984)

[17]Y Suzuki, et al, "Recent Developments in Picosecond Streak Camera Systems," Phil Trans Series A 298(1439), 295-302(1980)

[18]Y Tsuchiya, et al, "Universal Streak Camera," SPIE 491, 86-94(1984)

[19]T Y Tou and S Lee, "Multislit Streak Photography for Plasma Dyanmics Studies," Rev Sci Instrum 59(11), 2370-2374(1988)

[20]C B Johnson, et al, "A Magnetically Focused Photoelectronic Streak Camera Tube," SPIE 97, 56-61(1977)

[21]C L Wang, et al, "Microchannel Plate Streak Camera," SPIE 491, 82-85(1984)

[22]W Sibbett and W E Sleat, "A Photochron IIC Circular-Scan Streak Camera With CCD Readout," SPIE 674, 543-558(1986)

[23]K Brown, NASA/GSFC, private communication

[24] Thomas S, et al, " Improvements in Avalanche-Transistor Sweep circuitry for Electro-Optic Streak Cameras," Opt Eng 25(3), 465-470(1986)

[24A] Eberhardt EH, "Gain Model for Microchannel Plates," Appl Opt 18, 1418 (1979)

[25] ITT/Electro-Optical Products Division, Technical Note #TN114, 1970

[26] Earth Observing System (EOS), Background Information Package (BIP), Announcement of Opportunity #OSSA-1-88, "Part Four: Polar Platform Payload Accommodations Handbook," NASA/JPL (19JAN88)

[26A] Lieber AJ, et al, "Sub-Picosecond Proximity-Focused Streak Camera for X-ray and visible Light," SPIE 94,(1976)

[27] "Electro-Optics Handbook," RCA Corp, 1968, pg 10-8

[27A] Cromwell RH, "Toward Solving the Lost Photon Problem in Image Intensifiers," SPIE 627, 610-615(1985)

[28] E G Stassinopoulous et al, "METSAT Charged Particle Environment Study: Revised Edition, Method 2," GSFC X-600-87-4, AUG87

[29] Earth Observing System Background Information Package, Part Four: Polar Platform Payload Accommodations Handbook, Fig4-7

[30] K J Kaufmann, Hamamatsu Corp, Bridgewater NJ, personal communication

[31] ITT/Electro-Optical Products Division, Tech Notes #TN114 and #TN118

[32] Grove A S, "Physics and Technology of Semiconductor Devices," John Wiley and Sons, Inc, New York (1967), pp 191-195